SABANCI UNIVERSITY

Analysis on Micro Milling Dynamics and Stability

Submitted to the Graduate School of Engineering and Natural Sciences in partial fulfillment
of the requirements for the degree of Master of Science

Volkan ARAN
29/07/2011

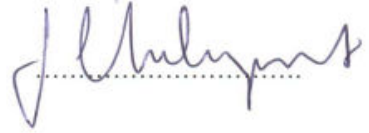ANALYSIS ON MICRO MILLING DYNAMICS AND STABILITY

Approved By:

Prof.Dr. Erhan Budak (Thesis Advisor)

Assoc. Prof.Dr. Ayhan Bozkurt

Assoc. Prof.Dr. Tonguç Ünlüyurt

Asst. Prof.Dr. Volkan Patoğlu

Asst. Prof.Dr. Bahattin Koç

Date
29.07.2011

To whom it may concern...

ANALYSIS ON MICRO MILLING DYNAMICS AND STABILITY

Volkan ARAN

Industrial Engineering, Master of Science Thesis, 2011

Thesis Supervisor: Prof. Dr. Erhan Budak

Abstract

Smaller sizes are becoming more and more necessary for industry. Literally, machining features less than one millimeter are called micro machining. Milling using small or mini tools is one of the most common manufacturing processes for production of precision products. As in the macro milling, milling with mini tools also suffer from well known unstable vibration problem which is called regenerative chatter. Chatter prediction models need certain process, tool and workpiece related information. Tool tip frequency response function FRF is the key input information for cutting dynamics and chatter stability analyses. The common method for determining macro tool tip FRF is the experimental modal analysis. However, in micro tools receptance coupling analysis is popular in the literature due to certain restrictions of experimental test method.

This thesis is focused on determining dynamic parameters of miniature milling tools by modal testing methods which are crucial to determine the stability characteristics of the micro flat end milling. An indirect modal testing method is presented. Also stability limit prediction with a conventional model is compared with experimental results. Various chatter detection methods and milling conditions are tested. In process chatter detection problems and modelling difficulties related with the miniature tool geometry are reported. Tool dynamics prediction is done with certain accuracy. Although the thesis study lacks from solid results in the stability limit prediction, discrepancy analysis of the test data are done and it is a first step for further studies.

MİKRO FREZE DİNAMİĞİ VE KARARLILIĞI ÜZERİNE ANALİZLER

Volkan ARAN

Endüstri Mühendisliği, Yüksek Lisans Tezi, 2011

Tez Danışmanı: Prof. Dr. Erhan Budak

Özet

Küçük boyutlar endüstri için gün geçtikçe daha önemli hale geliyor. Mikro frezeleme de 1mm altındaki hatların freze ile işlenmesi için kullanılan bir tabirdir. Küçük takımlarla ya da mikro takımlarla frezeleme hassas ürünlerde gittikçe daha çok kullanılan bir yöntemdir. Geleneksel takımlarla işlemede görüldüğü gibi tırlama ve işleme sırasındaki titreşimler mikro frezeleme işlemlerinde de önemlidir. Tırlama tahmini modelleri kararlılık limitlerini tahmin etmek için takım dinamiği ve kesme kuvveti modellerine ihtiyaç duyar. Takım ucu frekans tepki fonksiyonu işleme dinamiği ve kararlılık analizi açısından anahtar bir girdi verisidir. Geleneksel takımlarda frekans tepki fonksiyonu deneysel modal analizle bulunur. Mikro freze takımları için ise doğrudan modal analiz mümkün olmamaktadır. Testte yöntemlerinin sınırlamaları nedeniyle literatürde dinamik esneklik eşlenmesi metodu yaygındır.

Sunulan bu tez mikro freze takımların kararlılık limitlerinin belirlenmesi için gerekli olan temel parametrelerin modal test yöntemi ile belirlenmesine odaklanmıştır. Dolaylı bir ölçüm metodu önerilmiştir. Ayrıca deneysel ve geleneksel takımlar için geliştirilmiş bir modelle tahmin edilen teorik kararlılık limitlerinin mikroya yakın ölçekte takımlarla yapılan testlerle karşılaştırılmıştır. Çeşitli işleme durumlarında, farklı tırlama tespit methodları kullanılmıştır. Mikroya yakın ölçekte takımlar için işleme sırasında tırlama tespitindeki güçlükler tespit edilmiştir. Takım dinamiği dolaylı test yöntemiyle belirli limitler dahilinde ölçülmüştür. Kararlılık limitlerinde testlerle tahminler arasında büyük açıklıklar olsa da farklar analiz edilmiştir ve daha ileri çalışmalar için bir adım atılmıştır.

Acknowledgement

Chronologically, I should begin with my mother, father as the source of my existence. Thanks to them I was able to become what I am. There is no easy way to present gratitude towards them. My brother was the greatest supporter of me during my master years both in spiritual and materialistic ways. For example, without his car my second year would be far more miserable.

Erhan Budak was the main reason for me to come to Sabancı University. His vision and effort had created MRL. Thus the machining research which is subject to this thesis was possible. Additionally, his guidance and character shaped a huge amount of my thoughts.

All the people of the 1021 were great comrades. Thanks to them. Their patience to me was triumphant.

The people around MRL were my secondary advisors and helped me a lot. Thanks to them I was able to have precious technical conversations: Dr. Emre Özlü, Dr. L. Taner Tunç, Dr. Erdem Öztürk, Ömer Özkırımlı, Gamze Koca, Esma Baytok. Special thanks to Mehmet Güler and Süleyman Tutkun. (Mehmet abi, Süleyman çok teşekkürler.)

Table of Contents

List of Figures

List of Tables

CHAPTER 1   INTRODUCTION

The need for the small components continues to grow in many industries. Machining in micro size gives us new ways to accomplish old engineering missions. Machining features lower than one micron is called micro machining. Fuel injectors, medical implants, electronic circuit elements are some of our daily life products which contain micro features. Micro manufacturing gains more and more importance as our resources and energy becomes less. Milling using small or mini tools is one of the most common manufacturing processes for production of these parts. As in the macro machining, milling with mini tools also suffers from well known unstable vibration problem which is called regenerative chatter [1]. Chatter prediction models need certain process, tool and workpiece related information [2] [3]. Tool tip frequency response function (FRF) is the key input information for cutting dynamics and chatter stability analyses.

1.1   Introduction of the Problem

The common method for determining tool tip FRF is experimental modal analysis [1]. Impact hammer tests or excitation with a shaker are not feasible methods to in micro milling tools due to their fragile structure. Tool tip is generally too weak to excite without breaking or altering the modal parameters (which is matter when shaker is used). Therefore, analytical or numerical prediction methods are used in the literature for tool tip dynamic response. Namely, receptance coupling and substructure analysis (RCSA) using beam models are a successful analytical method to be used for miniature tools [4] [5] [6] Recent advances are in the direction of Receptance coupling analysis [7]. Finite element analysis is also used for prediction of milling tool dynamics as well as verification of the analytical predictions [8]. In addition to fast and accurate prediction methods, there is also a need for a testing method to identify miniature tool dynamics. In this thesis, an indirect measurement procedure using mode shapes is applied to miniature tool dynamics. Indirect FRF measurement methods are applied in various engineering applications [9]. Its limitations and capabilities are examined and presented in the second chapter.

Tool tip FRF measurement was the first challenge and the chatter detection is the second. Contrary to conventional size milling operations regenerative chatter detection literature is not mature enough in the micro mechanical milling. Various sensors are used and surfaces are examined for chatter signs detection. The results show that to have robust chatter detection mechanisms for micro milling a separate extensive study is necessary. In this thesis vibration marks on the surfaces are accepted as the most reliable chatter indicators as well as tool shank vibration spectrums.

The micro milling literature indicates that when all the effects (e.g. variation in the force coefficients run out [10], process damping [11], robust chatter stability [12], the gap between analytical stability lobes with zero order solution and real world test should not be more than %100 in the cutting speeds of concern. However, repeating tests and conditions showed that the discrepancy between expected and predicted stability limits can be as high as eight to ten times of expected limit. As a source of these differences first effects of tool run out is examined and the related results are presented.

Another phenomenon that affected the experimental procedure is sudden and premature failure of end mill's sharp corner. This phenomenon is observed in almost all tests and that made experimental procedure extremely complex. Measurements on broken tool edges showed that broken and blunt parts of the tools are in the order of the axial stability limits of the tool.

As a conclusion, a study on micro flat end mill dynamics is completed. Various conditions were covered in the tests. Selected tool type created practical problems due to its geometry. Also force measurement capabilities of the laboratory were insufficient to characterize the tool specific force coefficients. It is shown that tool vibration parameters can be found in acceptable limits. However, to achieve a robust chatter detection and prediction more study is required.

1.2   State of the Art

1.2.1   Mechanical Micromachining Process Boundaries

The State of art in the mechanical micro milling is summarized in 2000 for the first time by Masuzawa et. al. [13]. Masuzawa stated that reducing unit material removal and using higher precision tools enables micro machining. Unit removal (UR) concept was introduced by N. Taniguchi as 'processing unit' to explain the difference between micromachining and conventional machining [14]. UR is defined as the part of a workpiece removed during one cycle of removal action. UR can be expressed in volume, area or length dimensions based on the process. According to molecular dynamics simulation results mentioned by Masuzawa, [13] micro cutting theoretically can achieve 1nm UR. The practical and dominating limitations are on the cutter edge radius and machining tool equipment precision. Single crystal diamond has the lowest known edge radius and it can be used with depth cut in the order of hundreds nanometers. Resulting surface roughness may be around less than ten or around ten nanometers [15].

An interesting 5 axis precision micro machining example is done by Takeuchi et.al. [16] . They produced a copper Buddha statute whose head has a radius around 4mm. A single crystal diamond tool having a pseudo ball end shape is used. They achieved surface roughness values around 10nm.

Another extreme material removal tool was invented recently (2010) by IBM Research Zurich [17]. This tool is not a mechanical cutting tool (In fact, it is a modified atomic force microscope.). However the machine has the best equipment precision and machining time combination and UR in the current material removal state of the art. It is a 3-D nanolithography machine having 40nm lateral and 1 nm vertical resolution and 10nm UR.

1.2.2   Micro Milling Forces

Micromachining mechanistic cutting models are being developed since 1996. First Kim and Kim proposed [15] an orthogonal cutting model . They showed that clearence face forces have significant contribution to the total cutting force. Bao and Tansel [18] has one of the first micro milling force models. Their work presents a geometric improvement on the Tlusty and Macneil's model. This is the simplest model to be used in micromachining. Since feed per tooth to tool radius ratio is large actual chip thickness is different from conventional

model. Circular tool path approximation (i.e. The 3rd assumption of Tlusty and Macneil model) is changed and the rest is the same. An empirical analysis based on the mentioned force model is done by Liang et. al. [19] Latter paper gives a cutting force analysis based on conventional mechanistic exponential force models with chip thickness based on micro end milling model of Bao and Tansel. And results showed that macro miling force models are far from determining micro cutting forces for the tested conditions. J. Kotschenreuther et. al. [10] benchmarked 4 known metal cutting force formulae, namely Taylor, Kronenberg, Kienzle and Richter. They tested the mentioned models for micro cutting conditions. And they introduced calibration parameters for microcutting conditions. Their experiments showed results from which previously hardened zone will remain on the machined surface. So, hardened layers may accumulate on the surface and behaviour of this phenomenon is related with the edge radius over depth of cut value. But the general behaviour of this phenomenon is not described by them. Using chip thickness model of Jun et. al [21], Park et. al. developed another recent mechanistic force model which takes into the account effects of dynamics of the tool [22]. In their study cutting force is characterized by shearing and ploughing dominant regimes. Contributions of the regimes are predicted respectively. In the mentioned work, Kalman filtering is used for the force measurement data.

1.2.3   Tool Run-out in Micro End Milling

General milling tool run-out sources are explained in detail by Eugen Rivin [23]. Whole machine structure is analyzed in his work. Although, micro milling was not the subject but high speed milling effects are analyzed and summarized in this work. One of the initial works on run-out effects on cutting forces is done by Kline and DeVor (1982) [23]. According to authors, run-out in a section of milling cutter is determined with two parameters ρ and λ (i.e. locating angle and run-out offset w.r.t. rotation axes). And the mentioned work assumes no cutter tilt, which means that run out is same along the tool length. This paper [24] assumes linear cutting force model and run out is analyzed as a parameter which only causes variation on chip thickness. Circular tooth path approximation is accepted. Armarego et. al. [25] have also made similar assumptions with DeVor and a similar chip thickness model. Their work is based on the thin shear zone assumption and run out is determined with two parameters xi the locating angle and center distance. In this work, run out effects on rake and pitch angles are observed yet they are neglected. Circular tool path is used and run out effects are accepted as just change in radii of the teeth. Tansel et. al. [26] investigated a more precise

cutter path and they formulated chip thickness with tool runout and the main difference is this work includes feed rate effects thus trochoidal (i.e. especially cyclodial) tooth path is considered. The main focus is instantaneous chip thickness and change in the clearance angle is not considered. Afazov et. al. [27] recently modeled micro milling cutting forces using FEA and in their recent work [28] change in stability limits are analyzed. Tool run-out at high speeds and angle changes are not considered in their work.

1.2.4   Micro Tool Structural Dynamics

Dynamic characteristics of spindle structures are known to be important in milling. Regenerative chatter [2] surface location error [4] and tool life [23] are main parameters which are influenced by the machine tool stiffness or dynamic response of the tool tip. Analytical modelling of whole dynamic "tooling structure" (i.e. spindle, tool holder, tool, bearings, tool holder spindle interface, tool holder tool interface) is one of the approaches to determine tool dynamics or tool frequency response function (FRF). Analytical modelling mainly consists of three stages: beam modelling, receptance coupling and contact parameter identification. Receptance coupling substructure analysis on machine tool structures is studied by Schmitz et. al [29] [30] At the first they used Euler Bernoulli beams [31] and translational springs and dampers on the interface. Park et. al. [32] considered rotational degrees of freedom and Erturk et. al. [33] used Timoshenko beam solution (by Aristazabal Ochoa [34]) and rotational and translational springs and dampers on the interfaces and the study included whole structure model including spindle and bearings. Filiz et. al. used spectral Tschebychev technique for solution of Timoshenko beam equation (the original solution by Yağcı et. al. [35]). In a recent study Filiz et. al. has also considered the fluted section as a twisted beam and modified the method for twisted beams [36]. Kıvanç and Budak previously worked on the fluted section and modelled as beam with equivalent diameter [8]. Extraction of interface dynamic parameters (e.g. tool-tool holder contact stiffness and damping) is tedious and results are assembly specific. In practice, direct modal testing is still one of the best solutions to obtain tool FRF. However, direct modal testing is not practical or possible for miniature end mills. Impacting on micro end mills may damage the tool. Since tool is very small with respect to miniature impact hammer heads, proper hits needs precise positioning and timing. Furthermore, precise hits needs special mechanisms. Receptance coupling combined with impact tests are the one of the solutions to this problem.

Movahhedy et. al. [32] used tool blanks to identfy tool-tool holder interface dynamics. Another approach is using blank FRF's having rigidly coupling them with tool beam models [12]. These methods characteristically has signal to noise ratio (SNR) problems. And literature indicates that longer tool or blank lengths results in better SNR values. Tool tip FRF estimation methods, which are fed by impact test results, will be called indirect testing methods which are practically limited with test result quality (SNR).

1.2.5 Micro Milling Stability

When vibration assisted machining research is excluded there are not many publications on micro milling stability area. There are studies using macro milling stability formulations and micro milling force models or structural dynamics models [28]. Micro milling specific cutting process dynamics is studied by Park et. al. [11] In their previous work process damping effects on stability are considered in micro milling and tool structure is modeled with receptance coupling. In their recent study, uncertainties and changes in the dynamics and cutting coefficients in determination of chatter-free conditions in micro-milling operation are considered through the robust stability method. Their robust chatter stability method utilizes the edge theorem and the zero exclusion principle for taking into account changing parameters within a specific range [12] and also includes process damping effects.

1.3 Motivation

Micro milling is one of the cheapest and fastest and most flexible manufacturing processes for creating micro features. The micro machining equipments are being developed year by year. Currently, linear axis accuracies of average micro machining tools are around 1 micron. Cutting tool research is another research direction to have more durable and effective tools. Process research is one another path, having a precise machine and a proper cutter is generally not enough to manufacture the desired product. Dynamics of the milling tool is one of the main aspects that one should aware of. Chatter and other vibration related problems will cause problems like rough surfaces or tool failure. Predicting chatter limits and measuring tool dynamic characteristics are important to achieve desired micro products.

Literature is not rich enough to solve problems of the industry. For example a measurement method for the tool tip FRF is missing.

1.4 Objective

The main objective of this thesis is to develop methods to identify stable micro milling conditions for improved productivity and surface quality which can be obtained in micro milling processes. Determining stability limits are dependent on two main parameters in macro milling: cutting forces and workpiece/tool dynamics. In accordance with this, the first aim is to investigate methods for measurement or prediction of the micro tool dynamics. As a natural counterpart of this, analyzing effects of vibrations on micro cutting process is another important focus of this work. This is also extended to include investigation of chatter stability in micro milling as one of the major objectives in this thesis.

1.5 Contributions

Indirect measurement method for tool tip FRF is presented and limitations are shown. In process chatter detection problems of miniature end milling are detected. Vibration marks on both side surfaces and bottom surfaces of the machined workpiece are examined. According to the used chatter detection criteria, analytical stability limits were far below the detected chatter limits. Cause of the discrepancy is found as the difference between modeled geometry and the real geometry of the tool which are not controlled precisely and differ from tool to tool.

CHAPTER 2: STRUCTRAL DYNAMICS OF MINIATURE FLAT END MILLS

Machine-tool structure is very important for machining vibrations and resulting part quality. In order to predict process dynamics problems such as chatter limits or surface location errors, identifying dynamic parameters of tool tip is crucial. Although there are modelling approaches for micro end mill dynamic responses, a measurement method is not seen in the literature. An indirect modal test method will be presented and analyzed and for its limiting circumstances a receptance coupling method will be presented as a future work.

2.1 Indirect Modal Test for Miniature End Mills

Since impact testing or similar methods cannot be used for measurement of miniature tool dynamics, an indirect measurement method is applied. The structural system is assumed

to be linear time invariant (LTI), and the frequency domain formulations of the dynamic response are used. Since linear dependence is assumed among the parameters formulation is used for only around natural frequencies.
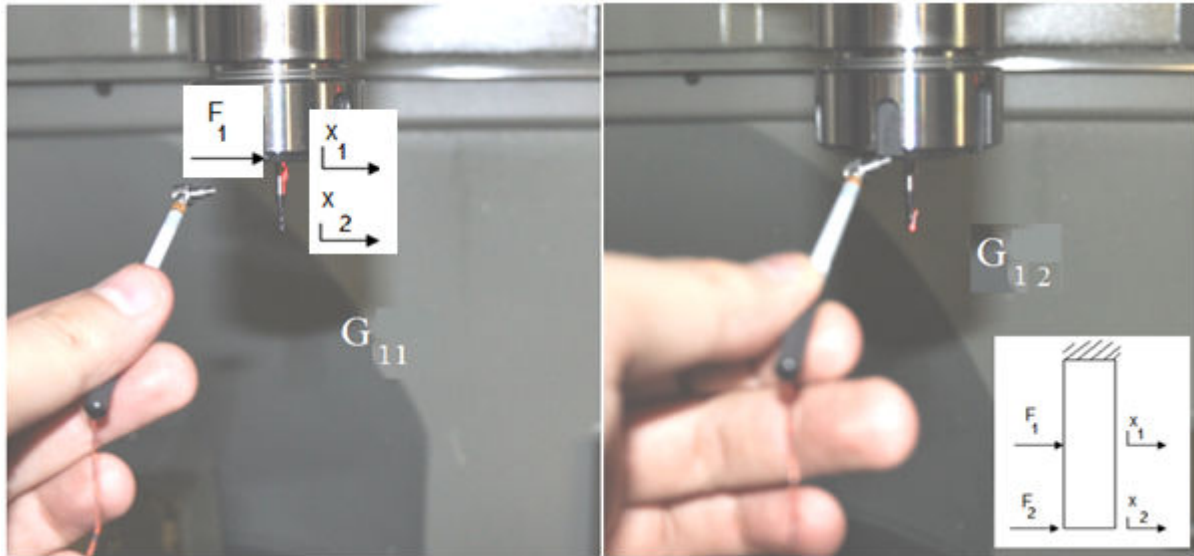
Figure 2-1: Inputs and outputs of the structural dynamic system

Considering the structural representation of the miniature tool shown in the right corner of the Figure Figure 2-1: Inputs and outputs of the structural dynamic system, the responses can be defined as follows in the frequency domain:

$$G_{11} = \frac{x_1}{F_1} \ , G_{12} = \frac{x_1}{F_2} \ , G_{21} = \frac{x_2}{F_1} \ , G_{22} = \frac{x_2}{F_2} \tag{2.1.1}$$

Where G_{11} is the transfer function of point 1 between force (F_1) and displacement(x_1). G_{12} and G_{21} are the transfer functions between force inputs from tool shank and tool tip respectively. G_{22} is the direct transfer function of the tool tip. .

From the above definitions and from the linear dependence assumption between parameters defined for point 1 and 2, following are obvious:

$$G_{22} = \frac{\dfrac{x_2}{F_1} \times \dfrac{x_1}{F_2}}{\dfrac{x_1}{F_1}} \qquad (2.1.2)$$

$$G_{22} = \frac{G_{21} \times G_{12}}{G_{11}} \qquad (2.1.3)$$

For a linear structure, G_{12} and G_{21} in equation (2.1.3) are the same [39] yielding

$$G_{22} = \frac{G^2{}_{21}}{G_{11}} \qquad (2.1.4)$$

Equation (2.1.4) indicates that the tool tip FRF can be determined by using the direct FRF at the tool's fixed end (G_{11}), and the cross FRF between the fixed and the free ends (G_{21}). This is a very convenient way to identify the tool tip FRF of miniature tools since the excitation at the tip is almost impossible.

Figure 2-2 Sample 2 dof mechanical system

In order to check limitations of the method consider a 2 degree of freedom basic vibratory system (Figure 2-2 Sample 2 dof mechanical system). The system has the following equation of motion:

$$\begin{bmatrix} m_1 & 0 \\ 0 & m_2 \end{bmatrix} \begin{Bmatrix} \ddot{x}_1 \\ \ddot{x}_2 \end{Bmatrix} + \begin{bmatrix} c_2 & -c_2 \\ -c_2 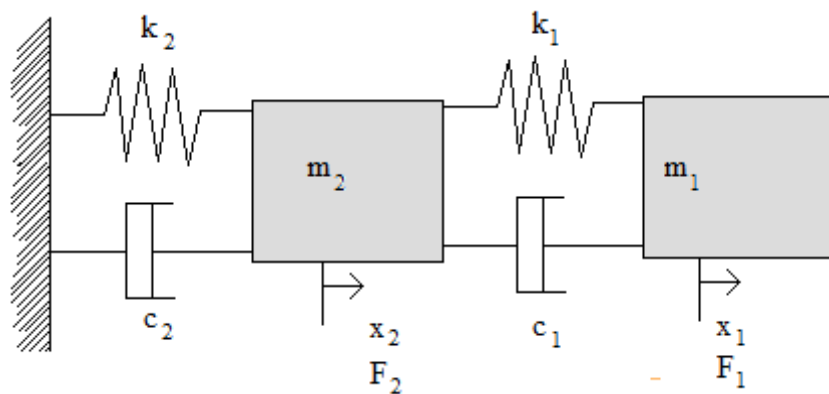& c_1 + c_2 \end{bmatrix} \begin{Bmatrix} \dot{x}_1 \\ \dot{x}_2 \end{Bmatrix} + \begin{bmatrix} k_2 & -k_2 \\ -k_2 & k_1 + k_2 \end{bmatrix} \begin{Bmatrix} x_1 \\ x_2 \end{Bmatrix} = \begin{Bmatrix} f_1 \\ f_2 \end{Bmatrix}$$

(2.1.5)

Let $x_i = X_i \, e^{j\omega t}$ and $f_i = F_i \, e^{j\omega t}$ where X and F are the displacement and the force magnitudes respectively and ω is the frequency in radians per second and t is the time. Then transfer function or frequency response function G becomes:

$$[-\omega^2[M] + j\omega[C] + K] \, X = F, \qquad G = inv[-\omega^2[M] + j\omega[C] + K]$$

(2.1.6)

Let the parameters of equation(2.1.5) be ordered as:

$$X = \begin{Bmatrix} x_1 \\ x_2 \end{Bmatrix}, \qquad M = \begin{bmatrix} m_1 & 0 \\ 0 & m_2 \end{bmatrix}, C = \begin{bmatrix} c_1 + c_2 & -c_2 \\ -c_2 & c_2 \end{bmatrix},$$

$$K = \begin{bmatrix} k_1 + k_2 & -k_2 \\ -k_2 & k_2 \end{bmatrix} \text{ and } F = \begin{Bmatrix} f_1 \\ f_2 \end{Bmatrix}$$

And G matrix is the same with equation(2.1.1).

Assign numbers to the related matrices (for this example numbers are selected as random values but in terms of order of magnitude close values to modal values of a miniature end mill in order to see clear and seperate modes) :

$$M = \begin{bmatrix} 0.55 & 0 \\ 0 & 0.37 \end{bmatrix}, \qquad K = \begin{bmatrix} 2.95e7 & -1.19e7 \\ -1.19e7 & 1.92e7 \end{bmatrix}, \qquad C = \begin{bmatrix} 0.0043 & -0.0042 \\ -0.0042 & 0.00063 \end{bmatrix}$$

G_{22} responses found from 2.1.6 and 2.1.4 for the described system, are compared at Figure 2-3. At the modal peaks values of the magnitudes are the same. Indirect method misses the anti-mode but that problem can be detected in a practical test application by checking G_{21} and G_{11} or by modal fitting to the these responses.
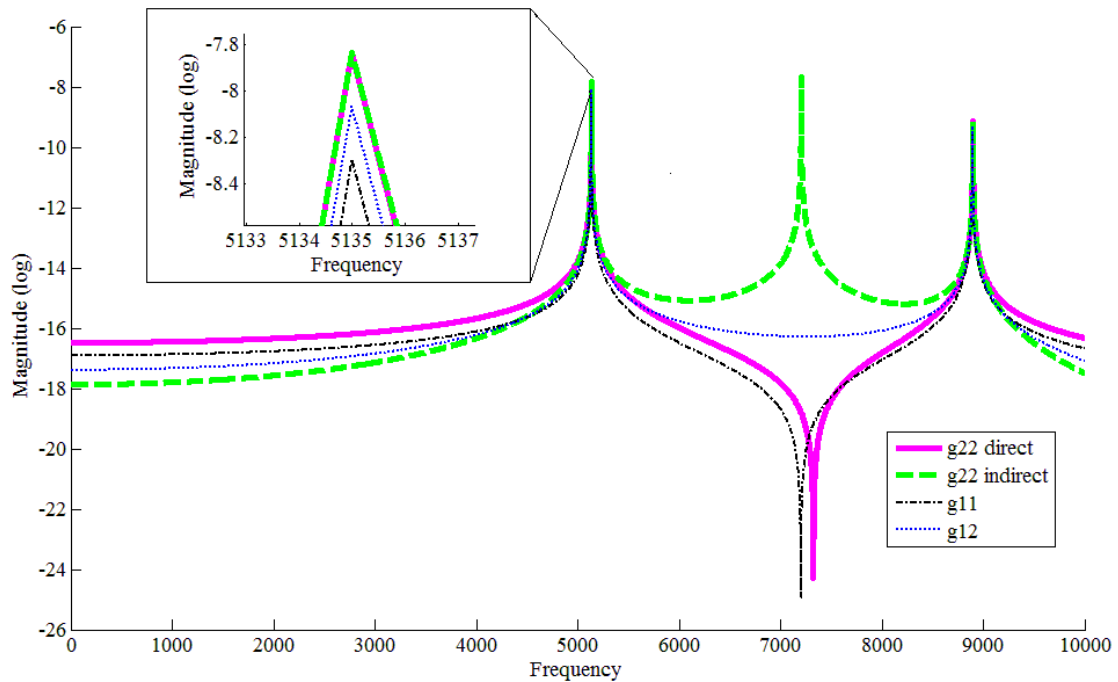
Figure 2-3 2 Dof System direct indirect G_{22} responses comparison

2.1.1 Experimental validation on standard end mills

Although the method described above is straightforward, its accuracy is verified with modal tests on standard sized tools where tool tip FRF can be measured directly. Implementation and verification of the method requires measurements and excitations at 2 points on the tool. The instrumented Modally Tuned® miniature impact test hammer (PCB 086D80) is used for excitation of the tool and the vibration response is measured with a Laser Doppler Vibrometer (Polytec IVS-300). Only one measurement is taken at a time, i.e. multiple measurements are performed on the tool to determine the direct and cross FRFs. The tool-holder assembly used in the tests is shown in Figure 2-4. The tool is a 10 mm diameter HSS end mill with 10 cm flute length. Results of the measurements are given in Figure 2-5.
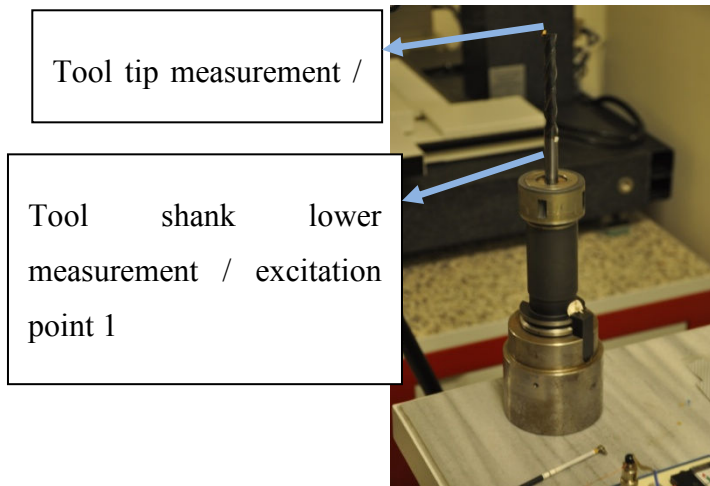
Figure 2-4: Tool-holder assembly for the test
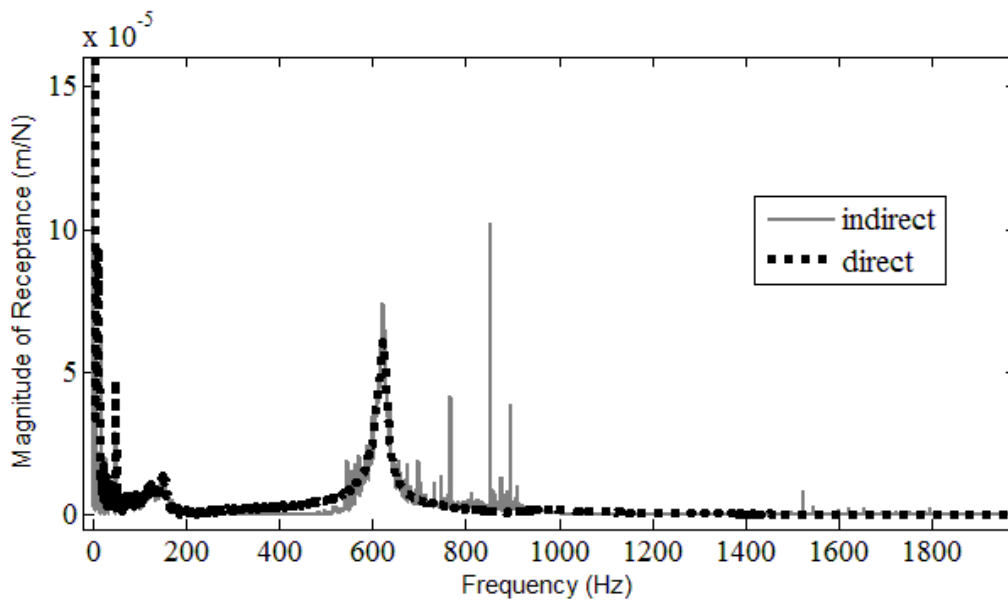
Figure 2-5 : Direct-indirect measurement FRF magnitudes comparison

Peaks between 700-1000 Hz on Figure 2-5show a noise amplification region. This numeric phenomenon will be discussed in depth in the next section. A simple solution for the noise amplification problem is to apply a modal curve fitting to measurements. Noise amplification problem is partially solved with single degree of freedom (SDOF) modal curve fitting method [40] by extracting the modal data and re-building the FRF. The results of this process are shown in Figure 2-6 for the same FRF shown in Figure 2-5.
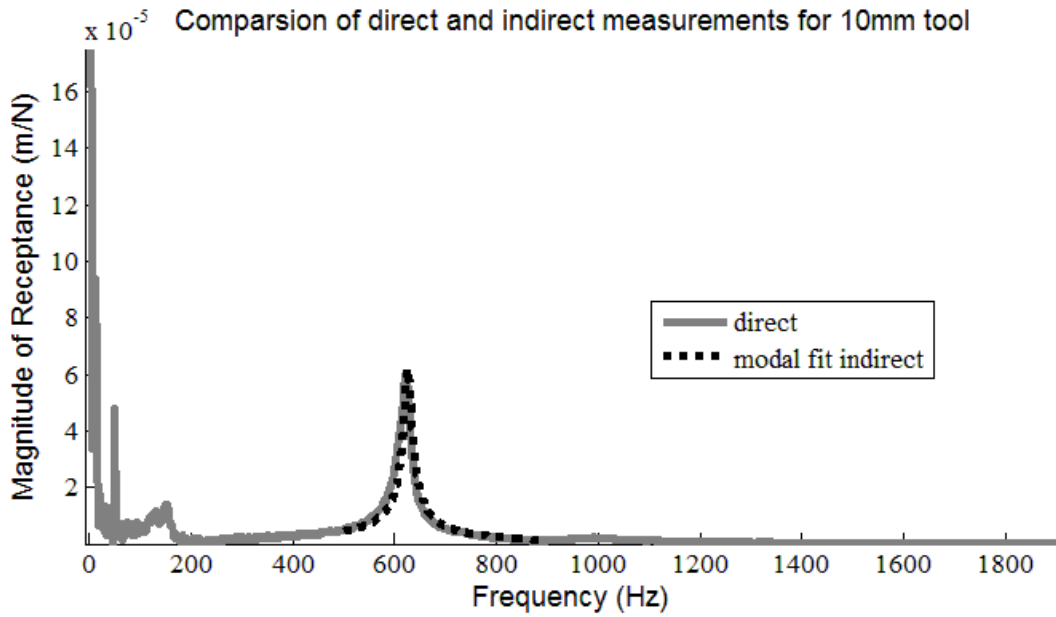
Figure 2-6 : Direct-indirect with modal fit measurement FRF magnitudes comparison.

Another Test is done with 28mm overhang 3mm tungsten carbide cylinder attached to the holder and machining tool. Impact hammer tests are performed and indirect measurement results are compared. Comparison graph is presented in the Figure 2-7. Modal peak results have 20% difference but tool tip was too flexible and obtaining direct transfer function was difficult and direct test results is not reliable as they are in the wider diameter tools mentioned before.
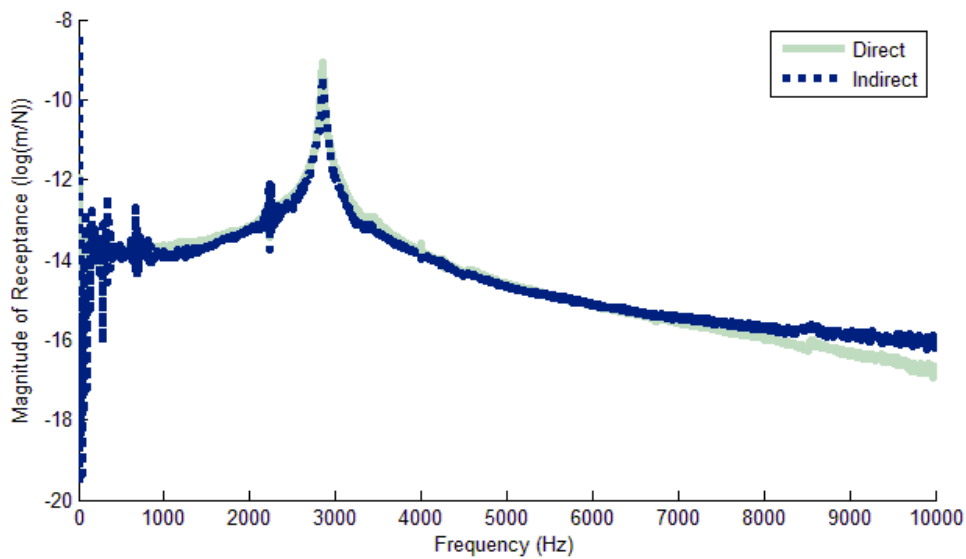
Figure 2-7: 28mm overhang 3 mm diameter cylinder direct indirect FRF comparison

13

2.1.2 Problematic Situations

It is important to find a rigid enough excitation point on the tool shank to have a fair energy distribution near the damped natural frequencies and a good coherence for both G_{11} and G_{21}. In terms of excitation power distribution and coherence these two transfer function do not have the same trends. Fig. 8 describes an example of this problem. The FRF of a 2 mm diameter carbide tool with 29 mm tool length is measured with Cutpro [10] software using the miniature impact hammer and the Laser Doppler Vibrometer (Polytec IVS-300) LDV. Three shank excitation points are selected which are separated by 10 mm from each other beginning from the tapered section of the tool. Overall the best results are obtained from point 3. (Black line in the Figure 2-8)
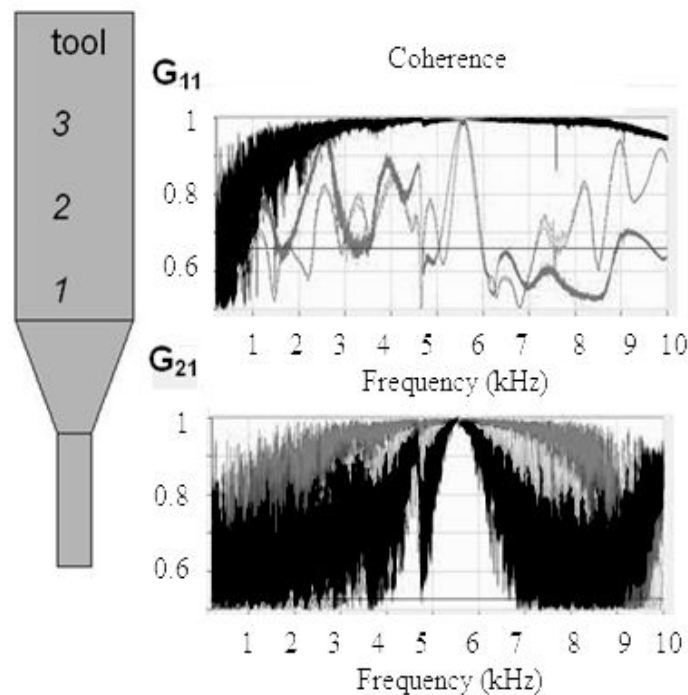
Figure 2-8: Coherence graphs of the three different excitation points. Light grey: 1, Dark grey: 2, Black: 3

The second problem is the noise amplification when G_{11} magnitudes are close to zero. This problem can be solved by the modal curve fitting to G_{11} and G_{21}. The regenerated indirect measurement from the modal curve fitted data helps to filter the noisy regions. The

method used for modal data parameter identification and reconstruction presented in section 6.1. It is known from tests with macro tools that modal fitting is successful in noise filtering (Figure 2-6). An example of the curve fitting to a miniature tool point FRF is presented in Figure 2-9 which shows the result of an indirect FRF measurement on a 1mm diameter and 20 mm long carbide tool connected to an air spindle. This is the worst noisy data of many test results, yet modal fitting can filter out the amplified noise. The indirect FRF indicates a mode at 5274 Hz due to the effect of the noise amplification around an anti-mode. However, if the same curve fitting method is applied to the direct measurement FRF's, i.e. G_{21} and G_{11}, and G_{22} is generated, a smooth result is obtained (Black line in the Figure 2-9). In the fitting approach dominant mode is at 5867Hz, and the previous peak at 5274 Hz due to the amplified noise does not appear.
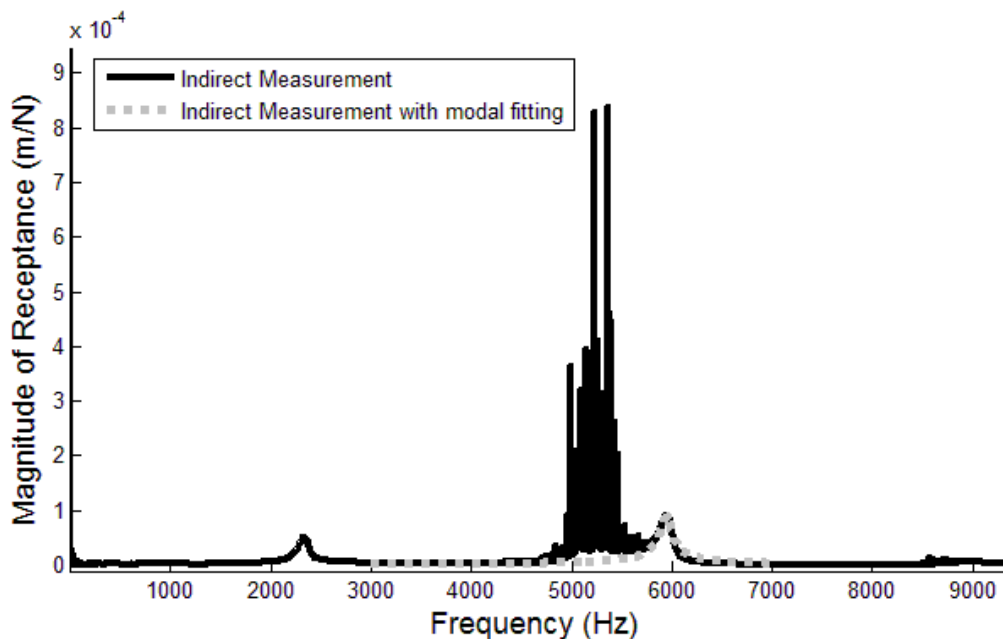
Figure 2-9: Indirect measurement FRF magnitude results for a 1mm diameter milling tool connected to an air spindle.

2.2   Indirect Receptance Coupling Analysis for Miniature End Mills

This part aims to develop a receptance coupling method which can be used as an indirect measurement technique. Receptance coupling substructure analysis is accepted as a prediction method in the literature mentioned above. However, author of this text believes that obtaining repeatable and reliable contact dynamics data is not practically possible at least for miniature end mills coupled with collets. Now consider basic two component rigid receptance coupling (see Figure 2-10):

Assume the whole structural dynamics is linear time invariant and a translational transfer function or FRF is defined as follows (lower cases correspond to component functions and upper cases correspond to assembly functions):

$$h_{1b1b} = \frac{x_{1b}}{f_{1b}} \tag{2.2.1}$$

In the beginning mid point frf formulation in terms of substructure responses will be obtained:
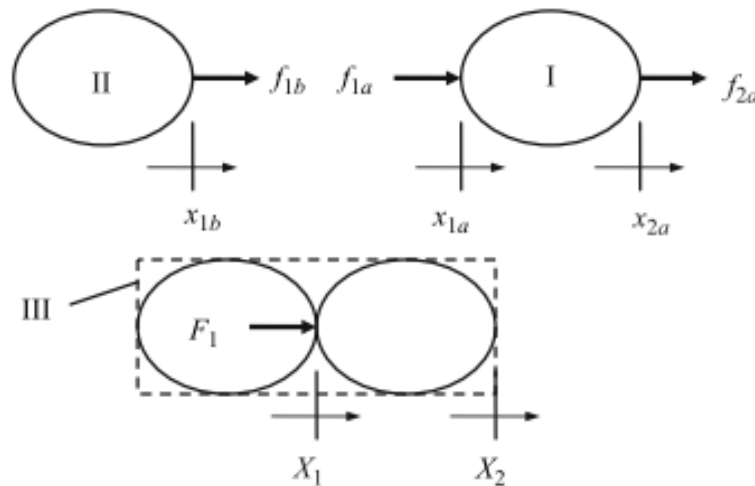
Figure 2-10: Rigid coupling of components I and II to form assembly III. The force F_1 applied to the assembly in order to determine assembly response H_{11}.

Receptance coupling formulations are based on two main set of equations: Compatibility and equilibrium. Compatibility equation is considered first:

16

$$x_{1b} = x_{1a} = X_1 \ , x_{1a} - x_{1b} = 0$$

$$h_{1a1a} f_{1a} - h_{1b1b} f_{1b} = 0 \tag{2.2.2}$$

Equilibrium is the second:

$$f_{1a} + f_{1b} = F_1 \ , f_{1b} = F_1 - f_{1a} \tag{2.2.3}$$

Now substitute Eq. 2.2.3 in 2.2.2 then solve for f_{1a} :

$$h_{1a1a} f_{1a} - h_{1b1b}(F_1 - f_{1a}) = 0 \ , f_{1a} = F_1(h_{1a1a} - h_{1b1b})^{-1} h_{1b1b} \tag{2.2.4}$$

$$f_{1b} = F_1(1 - (h_{1a1a} - h_{1b1b})^{-1} h_{1b1b})$$

And the contact point response becomes:

$$H_{11} = \frac{X_1}{F_1} = \frac{h_{1b1b} f_{1b}}{F_1} = h_{1b1b} - h_{1b1b}(h_{1b1b} - h_{1a1a})^{-1} h_{1b1b} \tag{2.2.5}$$

Define cross transfer function from point 1 to 2:

$$H_{12} = H_{21} = \frac{X_2}{F_1}, H_{21} = \frac{x_{2a}}{F_1}, H_{21} = \frac{(f_{2a} h_{2a2a} + f_{1a} h_{1a2a})}{(F_1)} \tag{2.2.6}$$

Substitute eq. 2.2.3 to f_{1a} :

$$H_{21} = \frac{f_{1a} h_{1a2a}}{F_1}, H_{21} = \frac{((h_{1a1a} - h_{1b1b})^{-1} h_{1b1b} F_1) h_{1a2a}}{F_1}$$

$$\tag{2.2.7}$$

$$H_{21} = ((h_{1a1a} - h_{1b1b})^{-1} h_{1b1b}) h_{1a2a}, \ H_{21} h_{1a2a}^{-1}$$
$$= ((h_{1a1a} - h_{1b1b})^{-1} h_{1b1b})$$

Now substitute Eq. 2.2.6) at Eq. 2.2.4 :

$$H_{11} = h_{1b1b} - h_{1b1b}[(h_{1b1b} - h_{1a1a})^{-1}h_{1b1b}] \qquad (2.2.8)$$

$$= h_{1b1b} - h_{1b1b}[H_{21}\, h_{1a2a}^{-1}]$$

$$H_{11} = h_{1b1b} - h_{1b1b}[H_{21}\, h_{1a2a}^{-1}]\,, \quad h_{1b1b} = H_{11}[1 - H_{21}\, h_{1a2a}^{-1}]^{-1} \qquad (2.2.9)$$

By equation 2.2.9 one can obtain the included effects of whole "spindle-machine" assembly at a virtually cut point on the tool shank (see figure below). Park et. al. [32] used two different tests to obtain tool blank FRF and this new equation reduces testing efforts. In the formulation one should see that the point 2 does not have to be an end point it can be an midpoint on a structure as well:

Let there exists a third body at the left of I (Figure 2-11):
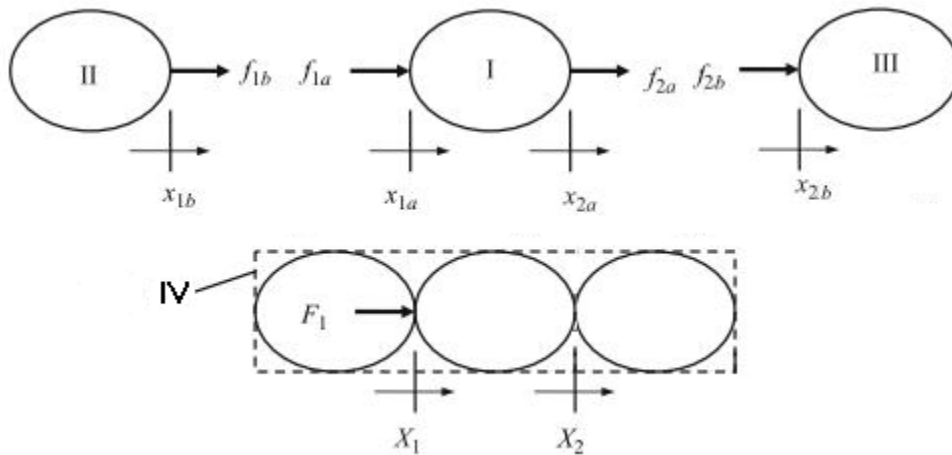
Figure 2-11 Three body assembly

Compatibility equation for the point 2,:

$$x_{2b} = x_{2a} = X_2\ ,\, x_{2a} - x_{2b} = 0$$

Since X_2 is still equal to x_{2a} equation 2.2.6 still holds.

In practice there can be two different application of this proposed formulation. They are described in Figure 2-12 and Figure 2-13 respectively.

Excitation at point 1 and measure the response at both tip and shank excitation points:
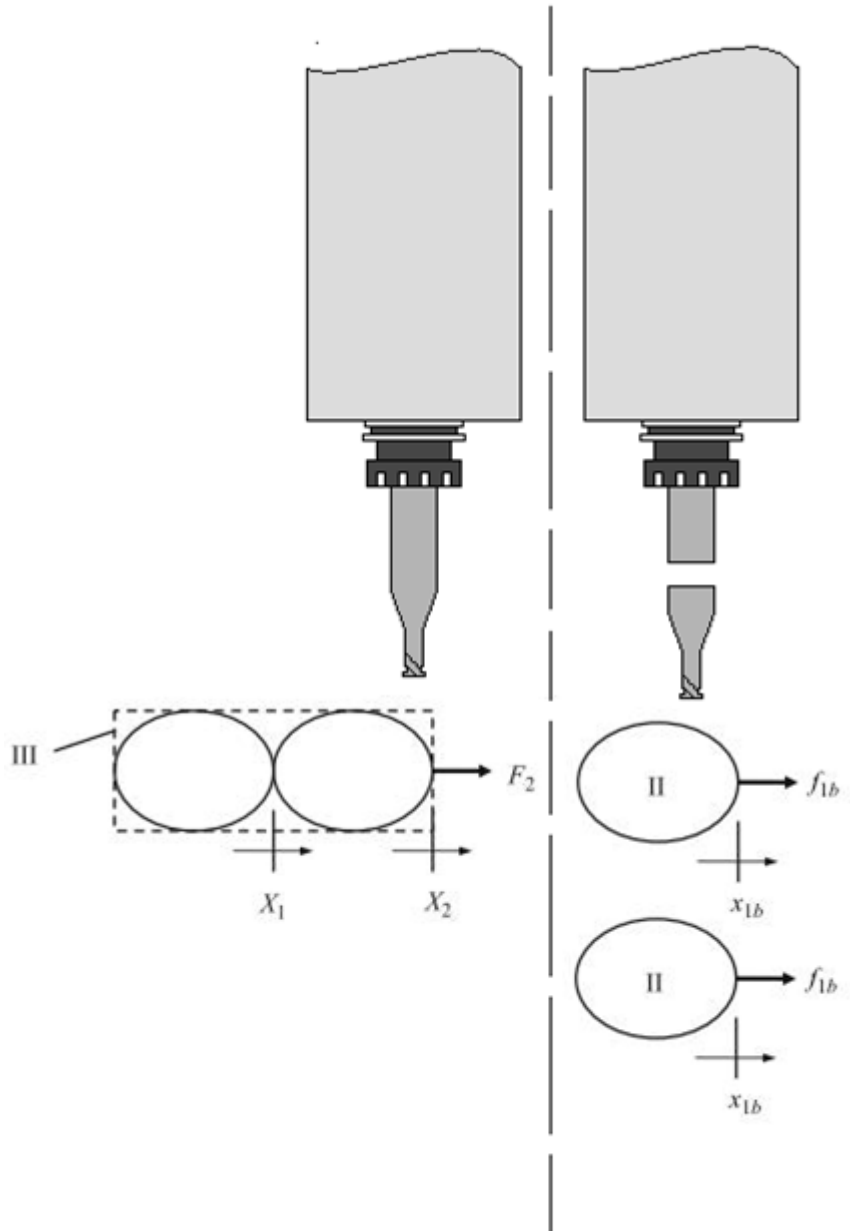
Figure 2-12 Receptance coupling model on machine spindle tool structure

Excitation at point 1 measure at another shank point:
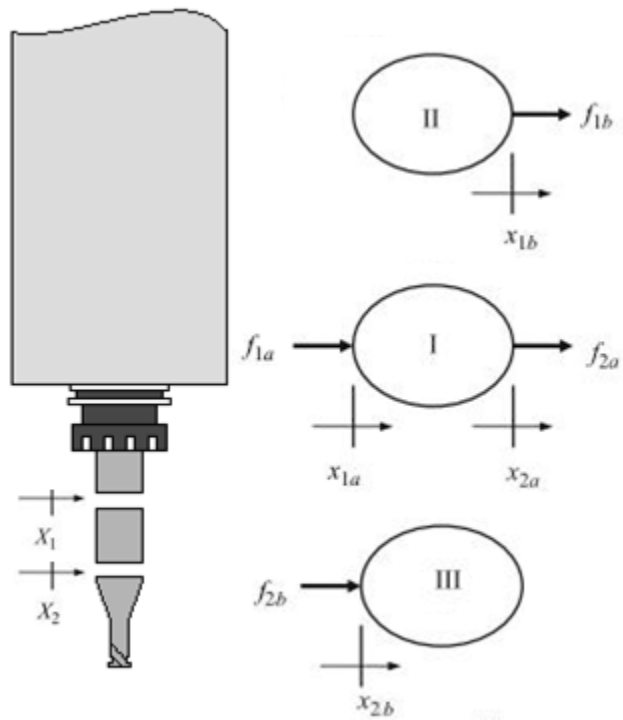
Figure 2-13 Three component model on machine tool spindle

CHAPTER 3: MILLING PROCESS DYNAMICS FOR MINIATURE END MILLS

This work is based on zeroth order solution of milling chatter stability limits from Budak and Altintas [2] [41]. The aim of milling chatter analysis is to determine stability limits in terms of axial depth of cut. As mentioned before there exists other models some of which are claimed to be more suitable for miniature-micro milling cases. Yet, according to the literature [12] [3] expected error from the applied stability model is not significantly high. The literature shows that the main differences between experimental and expected stability limits come from process damping and cutting force models. To reduce the process damping effects, higher cutting speeds are selected. Due to the limited measurement capabilities for measuring cutting forces, a suitable force model data were not available. But average forces are measured for lower spindle speeds than that of stability limits. are tested and compared with the implemented force model.

3.1   Milling Regenerative Chatter Model
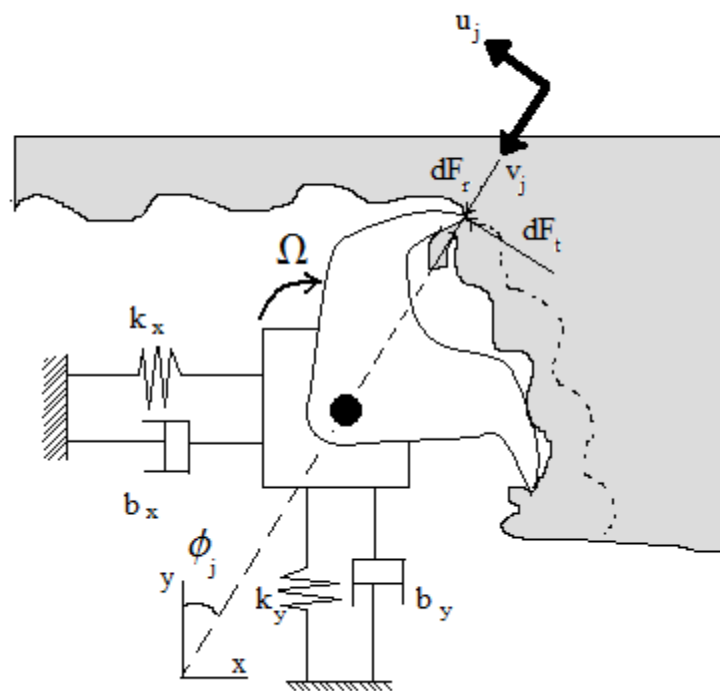
Figure 3-1 Milling chatter model

21

Milling cutter is modelled as 2 degree of freedom spring and damper vibration system on a plane as shown in Figure 3-1. Chip thickness is the one of the main geometrical parameters that creates cutting force. Milling machine, spindle, interface elements, tool and the workpiece are subjected to the dynamic cutting forces during a milling process. Dynamic displacement (i.e. vibration) of the tool and the workpiece creates variation or ondulation on the workpiece surface and on the uncut chip thickness. The ondulated surface will be subjected to the next cut (by next tooth or in the next revolution) and the tool and or the workpiece will be still vibrating. Process feeds itself to create thicker chips thus higher cutting forces and higher vibration amplitudes. This is called "regenerative" chatter or chatter instability in machining. Chip thickness variation can be represented as follows:

$$h_j(\phi) = f_t \sin \phi_j + \left(v_{j\mathring{c}} - v_{j\mathring{w}} \right) - \left(v_{j_c} - v_{j_w} \right) \qquad (3.1.1)$$

The feed per tooth f_t represents the static part of the chip thickness, and $\phi_j = (j-1) \phi_p + \phi$ is the angular immersion of tooth (j) for a cutter with constant pitch angle $\phi_p = 2\pi/N$ and N is the number of teeth as shown in Figure 3-1. $\phi = \Omega t$ is the angular position of the cutter measured with respect to the first tooth and corresponding to the rotational speed Ω (rad/sec). $v_{jc,w}^o$ and $v_{jc,w}$ are the dynamic displacements of the tool and workpiece in the chip thickness direction. Vibrations for the previous and current tooth passes, for the angular position ϕ_j. Since regenerative chatter is dependend on dynamic parameters or results of vibrations, the first term of chip thickness equation can be neglected. When dynamic displacements are represented in fixed xy frame, dynamic chip thickness becomes:

$$h_j(\phi) = \left[\Delta x \sin \phi_j + \Delta y \cos \phi_j \right] \qquad (3.1.2)$$

$$\Delta x = (x_c - x_c^o) - (x_w - x_w^o) \; ; \; \Delta y = (y_c - y_c^o) - (y_w - y_w^o) \qquad (3.1.3)$$

Where (x_c, y_c) and (x_w, y_w) are the dynamic displacements of the cutter and the work

piece in the x and y directions, respectively. The dynamic cutting forces on tooth (j)

in the tangential and the radial directions can be expressed as follows:

$$F_{t_j}(\phi) = K_t a\, h_j(\phi);$$
(3.1.4)

$$F_{r_{j(\phi)}} = K_r F_{t_{j(\phi)}}$$
(3.1.5)

where a is the axial depth of cut, and K_t and K_r are the cutting force coefficients. After substituting h_j from equation, the dynamic milling forces can be resolved in x and y directions as follows:

$$\begin{pmatrix} F_x \\ F_y \end{pmatrix} = \frac{1}{2}\, a\, K_t [A(t)]\{\Delta(t)\} \text{ where } [A(t)] = \begin{bmatrix} a_{xx} & a_{xy} \\ a_{yx} & a_{yy} \end{bmatrix}$$
(3.1.6)

where a_{xy} are the directional coefficients. The directional coefficients depend on the angular position of the cutter thus matrix "A" is dependent on time and periodic at tooth passing frequency. There are different approaches to the solution of the equation. Namely they are Multi-frequency [42] Single Frequency [2] and Semi-discretization [43] methods. This study is based on the single frequency solution or so-called zeroth order solution. The matrix will be expanded as finite Fourier series and only the "zeroth order" terms are kept. Coefficients take form of:

$$a_{xx} = \frac{1}{2}[\cos 2\,\phi - 2K_r\phi + K_r \sin 2\,\phi]_{\phi_{st}}^{\phi_{ex}}$$
(3.1.7)

$$a_{xy} = \frac{1}{2}[-\sin 2\,\phi - 2\phi + K_r \sin 2\,\phi]_{\phi_{st}}^{\phi_{ex}}$$

$$a_{yx} = \frac{1}{2}[-\sin 2\,\phi + 2\phi + K_r \cos 2\,\phi]_{\phi_{st}}^{\phi_{ex}}$$

$$a_{yy} = \frac{1}{2}[-\cos 2\,\phi - 2K_r\phi - K_r \sin 2\,\phi]_{\phi_{st}}^{\phi_{ex}}$$

Since increment terms are related to the previous cut profile (waviness of the surface to be cut), the equation of motion is a delay differential equation (T is the delay period) and transformed to the frequency domain. At the just initation of the chatter, excitation and response are at the chatter frequency. Equation 3.1.6 turns as follows:

$$F\, e^{i\,w_c t} = \frac{1}{2}a\, K_t\big(1 - e^{-i\,w_c T}\big)[A_0][G(iw_c)]F\, e^{i\,w_c t}$$

$$(3.1.8)$$

This leads to the eigenvalue problem:

$$det\big[[I] + \Lambda[G_0(i\,w_c)]\big] = 0, \quad G_0 = [A_0][G]$$

$$(3.1.9)$$

The eigenvalue can be expressed as:

$$\Lambda = -\frac{N}{4\pi}\, K_t a\,(1 - e^{i\,w_c t})$$

$$(3.1.10)$$

Stability limit for depth of cut "a" is sought and can be determined as follows:

$$a_{\text{lim}} = -\frac{2 \pi \Lambda_R}{N K_t} (1 + \kappa^2) \qquad\qquad (3.1.11)$$

Where $\kappa = \frac{\sin w_c T}{1 - \cos w_c T}$, $w_c T = \epsilon + 2 k \pi$, $\epsilon = \pi - 2k \psi$, $\psi = \text{atan } \kappa$, $n = \frac{60}{NT}$

Calculated limits are used for creating "analytical stability lobes". Limit axial depth of cut is plotted against rotational speed of the spindle creating curve of stability limit. It is a chart indicating stable zone below the curve.

The zeroth order solution lacks of accuracy for low radial immersions yet following test results show that there are practical problems far beyond of this numeric roughness. As an example of difference between multifrequency and zeroth order solution see the Figure 3-2 [41]. As shown in the figure, absolute limits are the same and there exists an additional stable zone (will be called lobes afterwards.) in the multi frequency solution which is a further expansion to the matrix "A" by including the higher Fourier components of the directional coefficients.
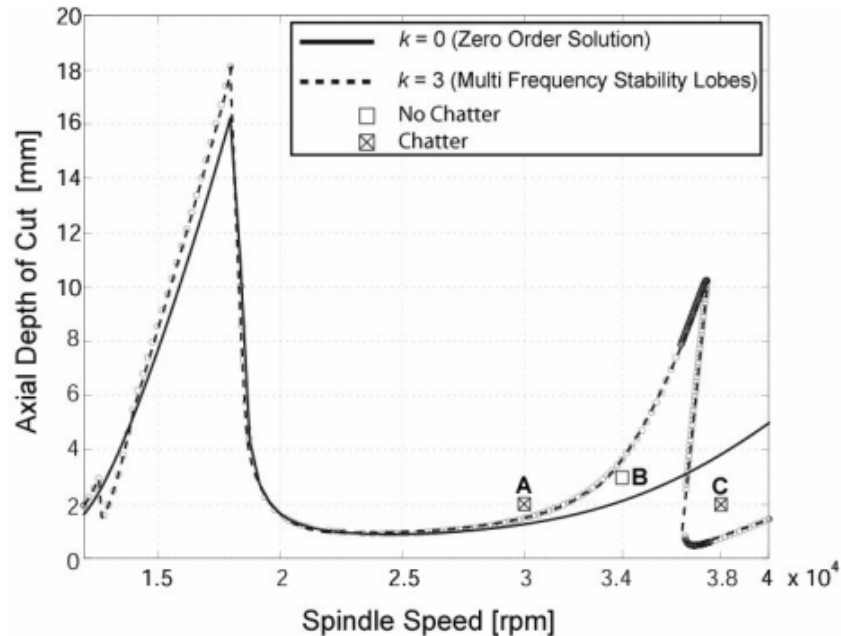

Figure 3-2 Comparison of single and multi frequency solutions [41].

3.2 Chatter Detection and Model Verification Experiments

The indirect measurement method of the tool tip FRF finds its application in chatter prediction. This part of the thesis presents applications and observations based on the presented indirect measurement method and the analytical stability model.

3.2.1 Milling Stability Tests

Milling stability tests were done in two ways: in the first way a set of adjacent step cuts are taken. (i.e. a series of cuts having constant depth of cuts, spindle speeds and feed rates.). The second is a ramp cut: An inclined surface is cut in determined speeds and feed rates with varying depth of cut. The most significant results will be presented. These sets are picked from many experiments, the full list can be found in the Appendix.

In generation of the stability diagrams for the first two sets, the tool is assumed to have symmetrical dynamic properties, and thus FRF's in x and y directions are assumed to be the same. Figures 3-5 to 3-9 present the test conditions used for a 2mm flat carbide end mill with two flutes and 29mm overhang length. The workpiece is an aluminum alloy, 7075T6. Cutpro9 [44] is used to create stability lobes. The force coefficients used in the software were verified by comparing the simulated and measured forces. Validations of forces are tested at lower speeds than stability test conditions (because of dynamometer sensitivity and frequency limitations) Tests conditions will be described hereafter. Best agreement is seen at slot milling conditions at 5000rpm (Figure 3-3). However for lower immersion conditions measured forces has different characteristics. (Figure 3-4) This will be discussed in detail in the next chapter.
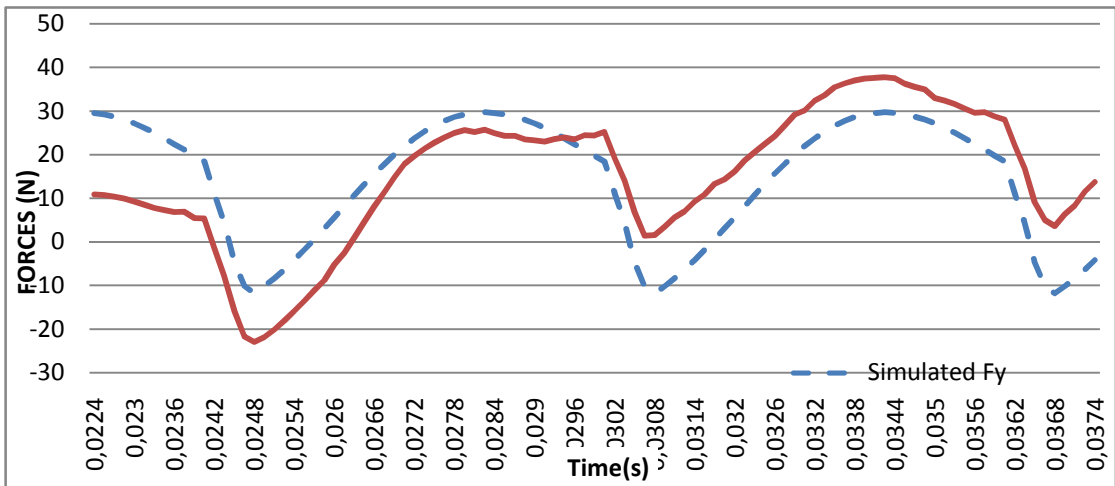
Figure 3-3 Comparison of cutting forces (slot milling)
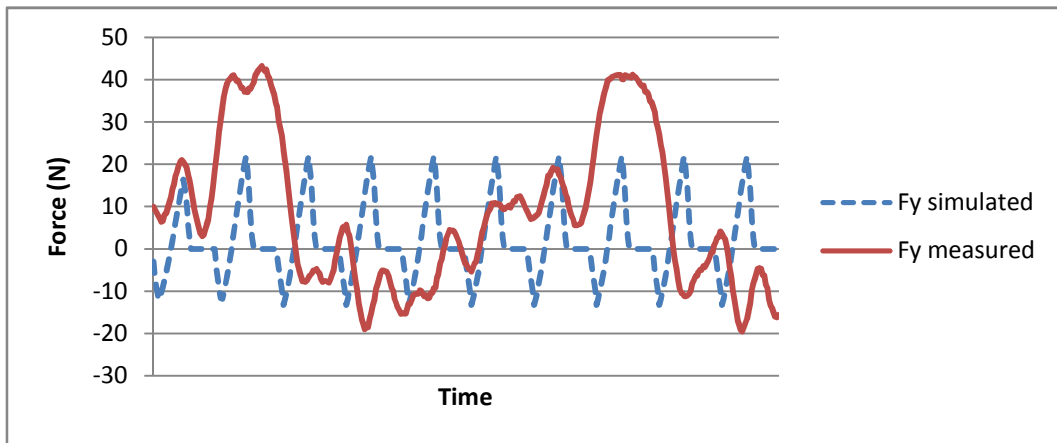
Figure 3-4 Comparison of the cutting forces (half immersion)

Three sets of chatter stability tests are done with same tool and the workpiece. At the first two sets the radial immersion was 100 micron and resulting stability diagram is shown in the Figure 3-5.

During the tests, acoustic emission (AE) sensor (Figure 3-5) (Physical Acoustics Corporation Nano30 [45], [3]) and a microphone (Figure 3-5) are used to collect data. Signals are acquired at 200 kHz with NI DAQ board. Amplifier is used for microphone and AE sensor is directly connected to the board.
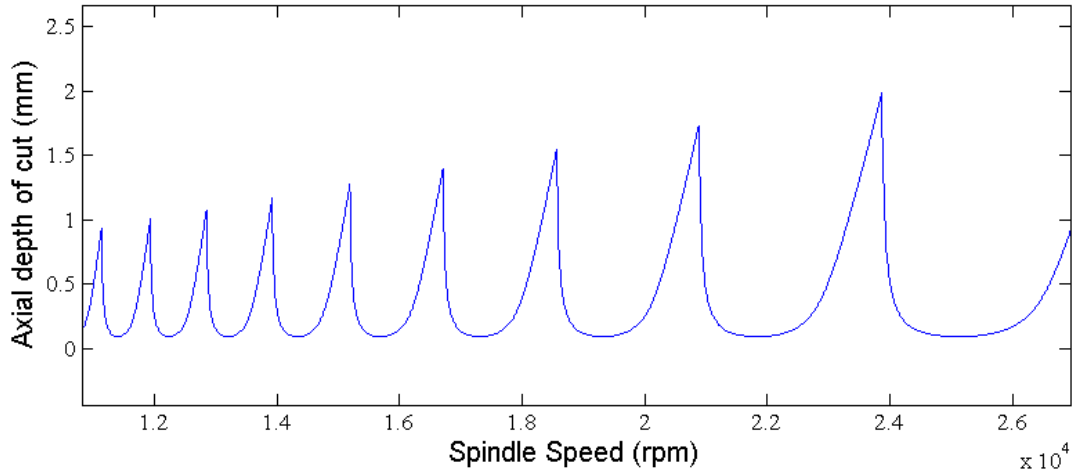
Figure 3-5: Stability diagram for 7075T6 aluminum with 2 mm diameter tool, 40 micron feed per tooth and 100 micron radial immersion.

3.2.2   Rigid Workpiece Adjacent Step Tests
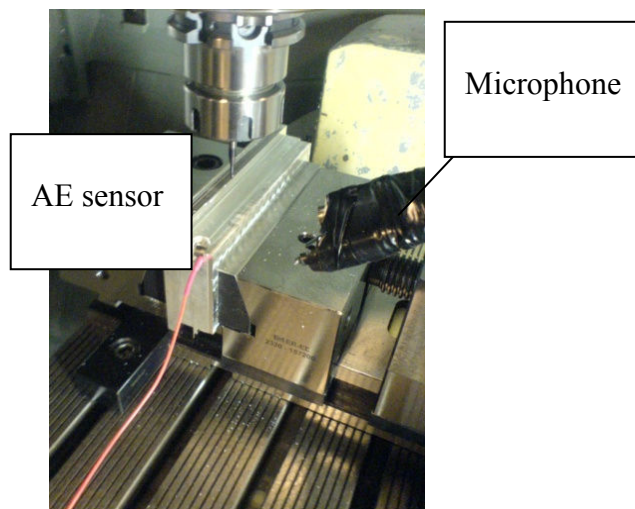
Figure 3-6: Test setup for low radial immersion chatter tests

Although it is known that for the lower radial immersions multi-frequency chatter models are more accurate, experimental stability limits are sought. Since lower radial immersions results in higher stability limits experimental detection was assumed to be easier. Two of test conditions will be presented here. Tests are conducted with a 2mm tool and 7075 aluminum workpiece. Both sets of tests are done with 0.1 mm radial depth with 0.04mm feed

per tooth. Spindle speeds discriminates the two sets of tests. Analytical stability limits for the test conditions are shown in the Figure 3-5. Results of the first set are shown in the Figure 3-7.
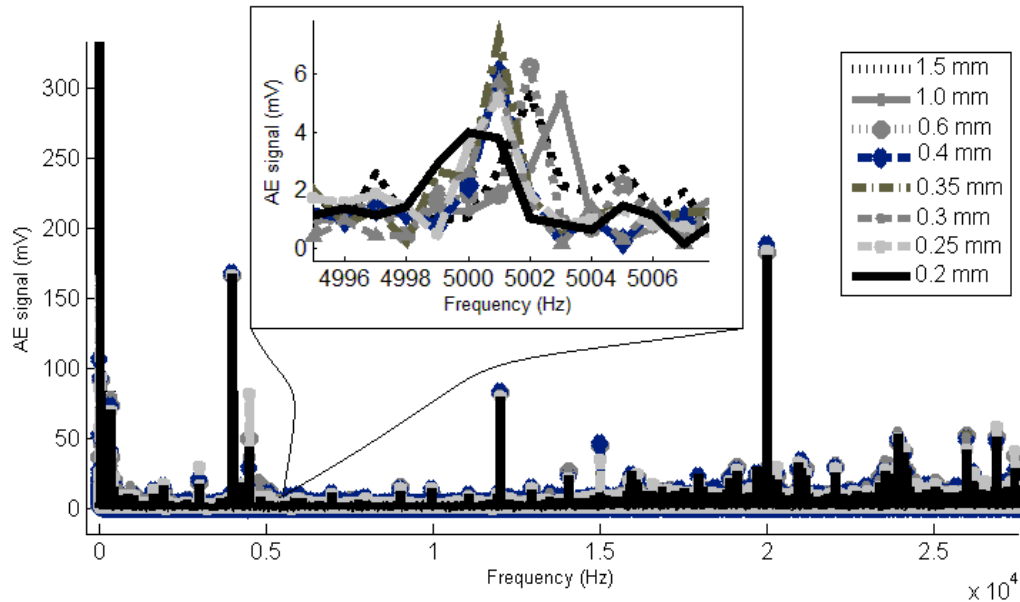
Figure 3-7 Spectrum of the AE signal for first set at 10250rpm

The detection of chatter has proved to be very difficult, in fact impossible using the sensors used in the tests. In the first set of the tests, the stability limit was tried to be detected. The observed chatter signs shown in Fig. Figure 3-7 and Figure 3-8 were weak and inconclusive. Although there are other possible causes (such as the outside noise changes between tests) 7 lines (i.e. data lines from 0.2mm to 1.5mm) of the 8 total data shows similar tendencies (up to 1mm) at the expected chatter frequency and this may be accepted as instability.

30
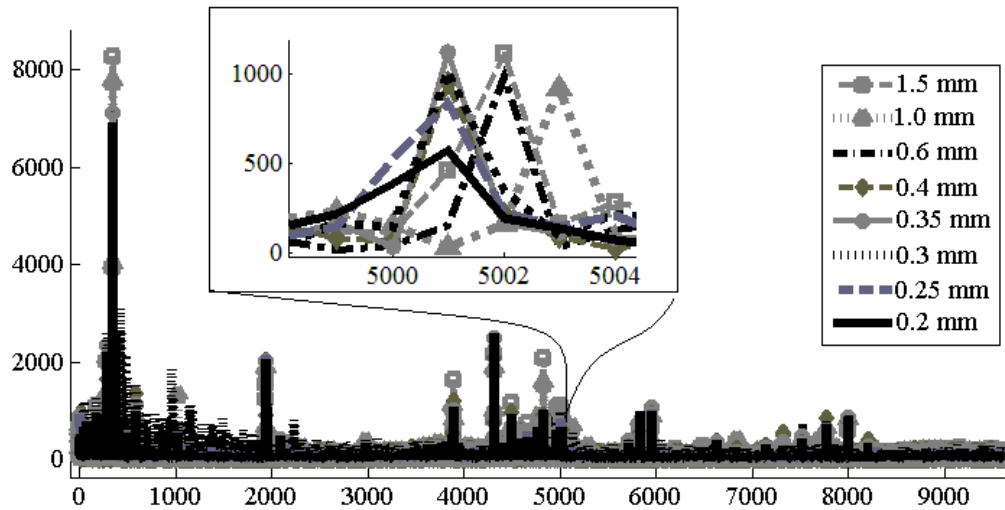
Figure 3-8 Spectrum of the AE signal for first set at 16600 rpm.

Second set of tests whose parameters are the same but the they are conducted using the same tool at a higher speed of 16600 rpm. Stability tests based on the analytical stability diagram given in Fig. 7 were carried out. Sudden change in the signals given in **Figure 3-9** shows signs of instability but these are not seen in the expected chatter frequency since they occur at a lower frequency of around 4930 Hz. Transition to the possible unstable condition is seen after data 4 which corresponds to 1mm depth where the expected stability limit is 1.13 mm .
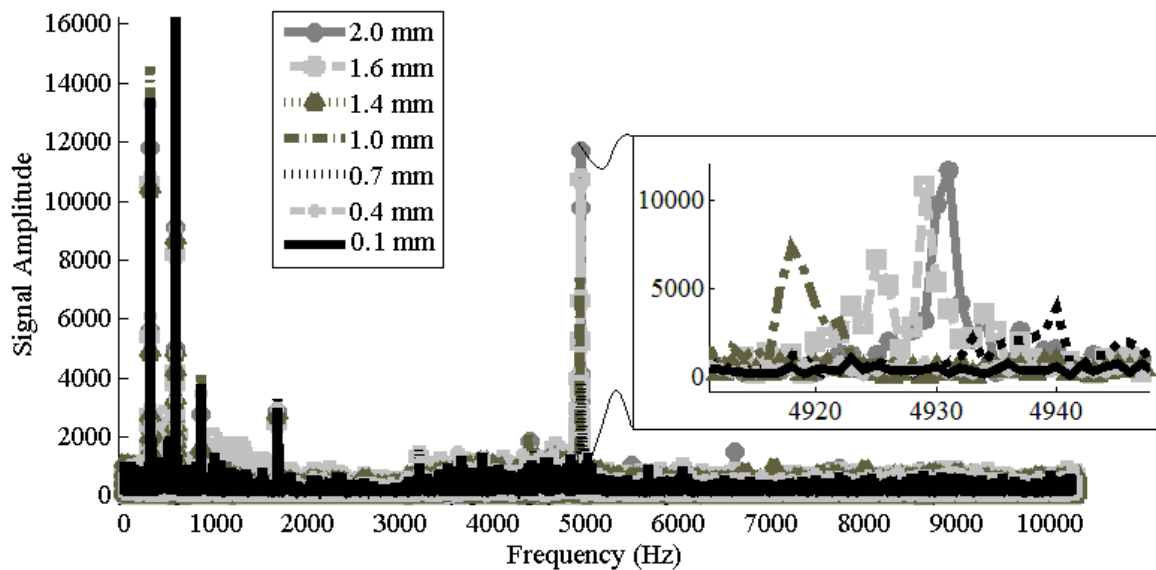
Figure 3-9 Spectrum of microphone signal for tests 1-7 in Table 2.

3.2.3 Flexible Workpiece Tests

Figure 3-10 Flexible workpiece setup

Another set of tests done with flexible workpieces. As can be seen from the previous figures SNR values and total vibration amplitude on the workpiece is small and that makes it hard to detect chatter signals. A flexible workpiece designed with the help of FEA and impact hammer tested (**Table 3-1**). Workpiece is selected to have higher modal stiffness values and higher damped natural frequencies than tool itself. Thus this design is assumed to result as tool vibration will be effective on the workpiece and tool chatter stability limits will not change. However results were not as expected. No tool chatter observed and not any tool frequency can be detected (which can be explained as attenuation of tool frequencies but it was not expected with predefined dynamic parameters).

Table 3-1 Dynamic properties of designed workpiece and the tool used in the test.

Dynamic Properties	Workpiece	Tool
Natural Frequency	6521 Hz	5561 Hz
Modal Stiffness	1.06E7 N/m	5.55E5 N/m
Damping Ratio	0.46 %	0.18 %
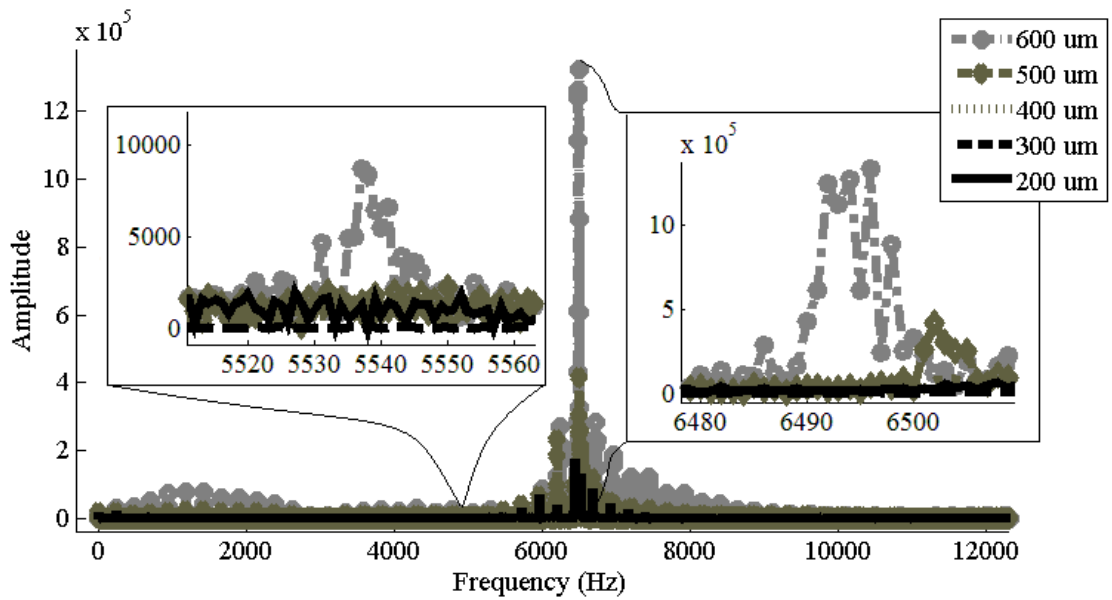
Figure 3-11 Spectrum of LDV signal (spot on workpiece)

3.2.4 Chatter Marks on the Surfaces

Third set of tests are aimed to see effects of higher depths which are far above the stability limits. For these experiments the same tool and the workpiece are used, but the overhang length was set as 25mm. The indirect measurement modal parameters of the tool were determined as follows (x direction/ y direction): damping ratio: 0.0046/0.0042, stiffness: 1.4663/1.4487 N/um, damped natural frequencies: 8080/8047 Hz. The stability diagram generated for this tool is shown in Figure 3-12. After the tests the bottom surfaces are inspected for chatter marks.
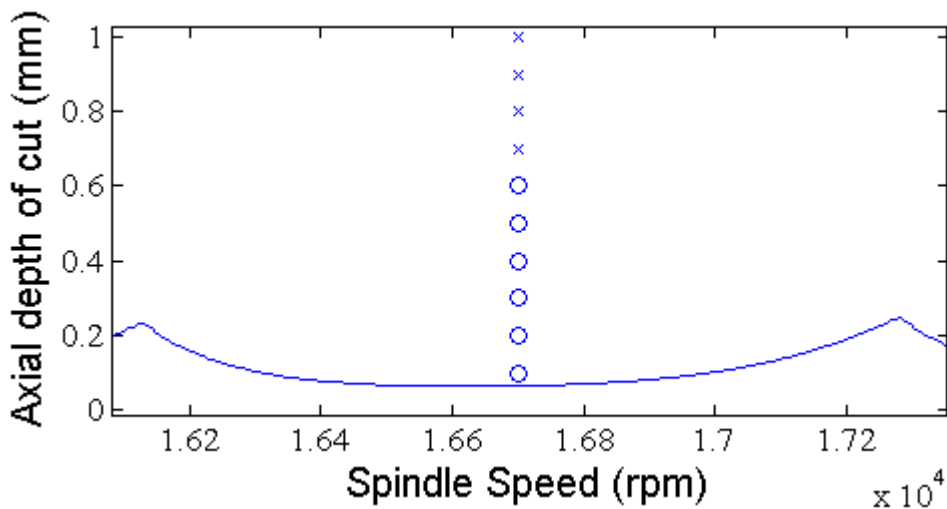
Figure 3-12: Stability diagram around 16000rpm for 7075T6 aluminum with 2mm diameter tool, 40 um feed per tooth and 1 mm radial immersion. (X: clear distortion on feed marks, O: not a clear distortion.)

In order to see the chatter marks on the surface several depths were tested at 16 700 rpm. The predicted stability limit is about 100 um as it can be seen from the diagram. The tests were started at 100 um axial depth of cut, yet not clear vibration signs were observed. As seen in Figure 3-13, there is a transition in the surfaces and distortion of feed marks near 800 um. This is much higher than the predicted stability limit which indicates a discrepancy and difficulty of chatter detection with miniature milling tools. Thus, the stability of milling process with miniature tools needs further investigation

34
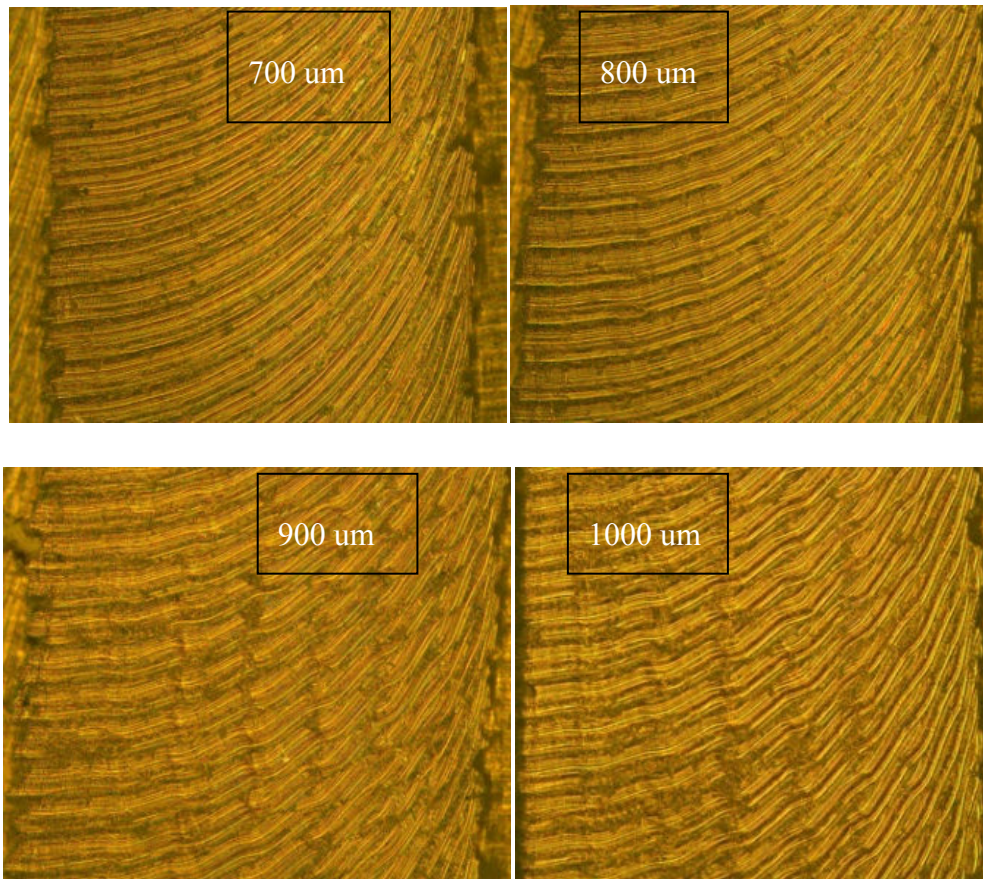
Figure 3-13 Microscopy photos of machined bottom surfaces during the tests. (Radial depths of cut are 1 mm. The pictures show bottom surfaces of 1mm wide steps.)

Another set of tests are done with inclined workpiece. Since estimated absolute stability limits are very low, ramp test method is found suitable for half immersion cutting conditions. From literature [4] and time domain simulation analyses its known that an average of five rotation of cutter is enough to develop regenerative instability. 5% inclination is machined on test workpiece first and inclined workpiece cut horizontally at 16000 rpm and 40μm feed per tooth. The tool has same properties with the 2mm tool described before and a new tool is used. Stability limit is expected around 40μm yet surface examinations showed that vibration characteristics change around 300μm and this is accepted as edge of instability. Change in the surface marks are interpreted as changing of the forced vibration frequency to the chatter frequency. Dr. Schneider WM-400 microscope is used for surface examinations shown in the Figure 3-14. Number of waves on the feed marks is between 6 and 7. Since this is a half immersion condition it turns out 24-28 waves in a period at 16000 rpm. These waves can be interpreted as a result of structural vibration of tool at 6-7.5 kHz. This band contains both chatter and natural frequencies of the tool. Expected chatter frequencies are around 7180 Hz. Change in the wave pattern can be seen in the following figure at the Figure 3-14.

35
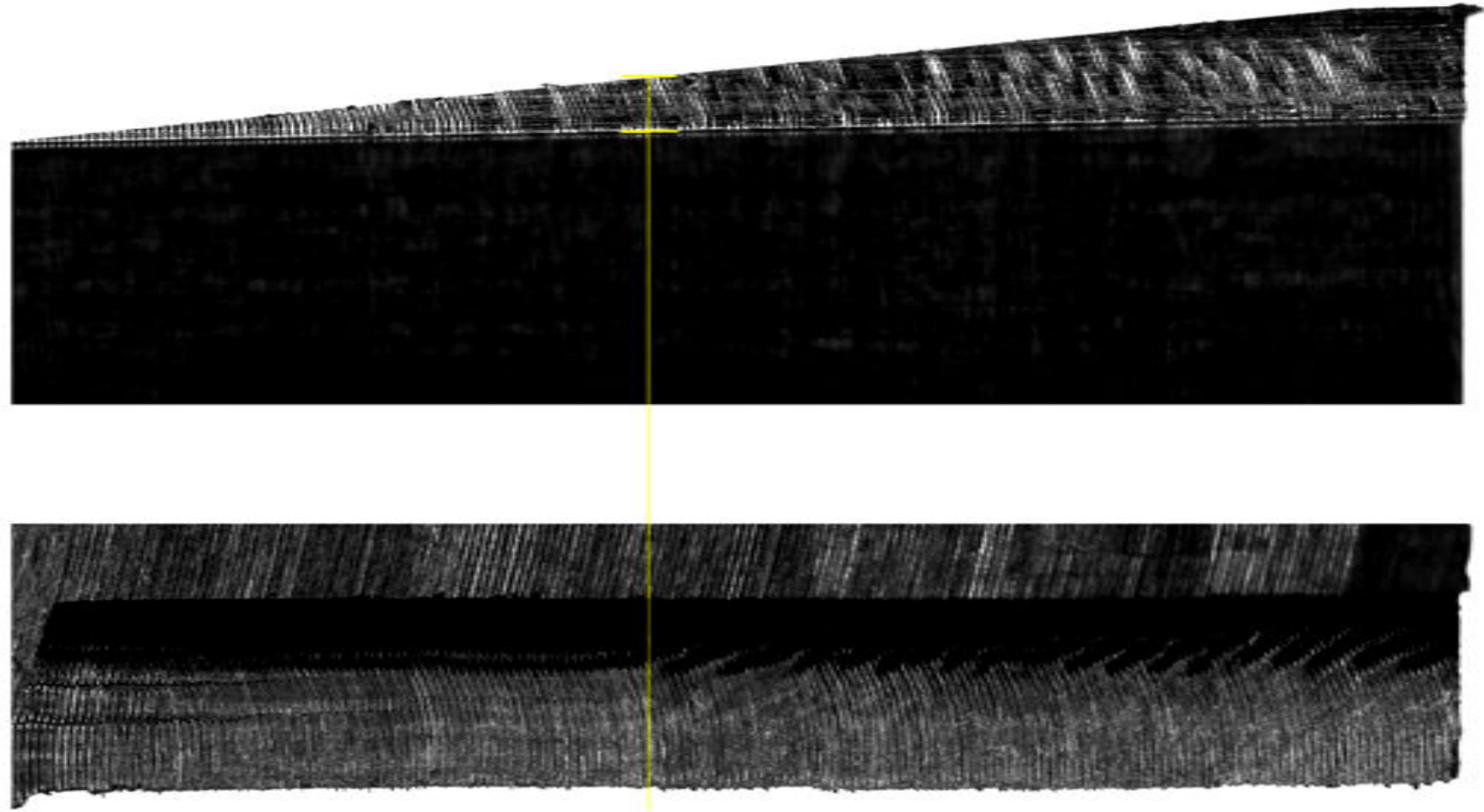
Figure 3-14 Ramp test surfaces from side and top views and stability limit

CHAPTER 4: ANALYSIS ON REASONS FOR DISCREPANCIES BETWEEN EXPECTED AND EXPERIMENTAL STABILITY LIMITS

4.1 Observations on Tool Geometries

As a source of lack of accuracy in the stability limit prediction, the tool geometry could be one of the main actors. Used and new tool geometries are examined and some problems related with the tool manufacturing method are observed. These observations are in parallel with some of the results reported in the literature [46]. Fang et. al. found that classic fluted end mill geometry is too weak for micro cutting and premaute chipping of cutter edge very likely occur.

Tool geometry problems can be classified in two different categories: design related problems and in-process failure problems. Design based problems are caused by second rake face. In standard milling definitions [1] flat end mill modelled with sharp end and constant helix. As can be seen in the Figure 4-1 miniature flat end mills have another face. Also in the side view change in the helix angle can be seen.
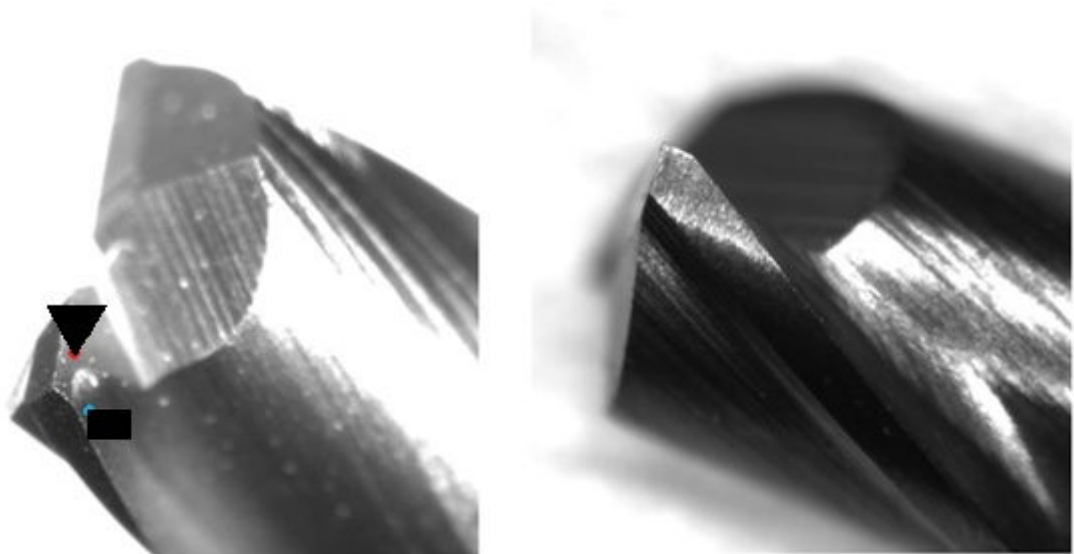
Figure 4-1. Unused tool and triangle signed face 2nd rake face. Rectangle dotted face is the standard rake face.

Another design or manufacturing related problem of the cutting tools is flute asymmetry. This may cause the imbalance of the tool which may change the process dynamics at the higher speeds. And its seen that run-out mainly caused by this imbalance (Figure 4-2).
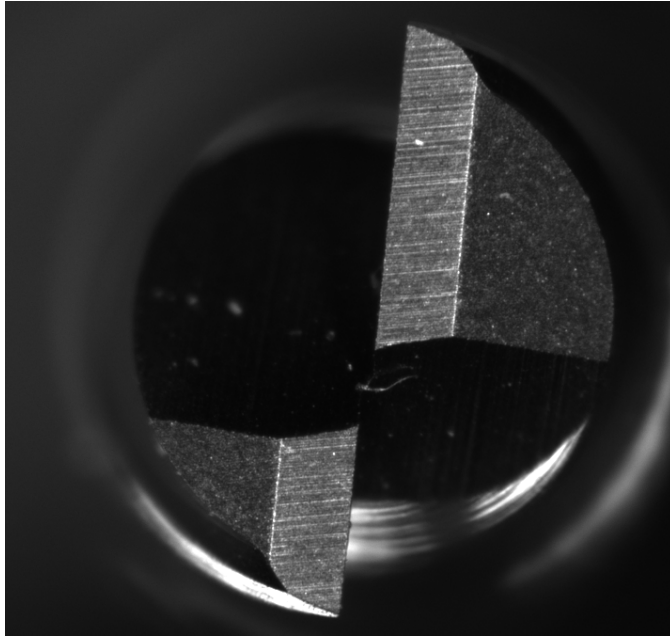
Figure 4-2: Asymmetric flute (bottom view of a 2mm milling tool)

Another tool geometry problem for modeling is chipping of cutter corners. Certain brand tools have a less 2nd rake face areas. Not having a 2nd rake face tool edge becomes very weak which is expected by Fang et. al. [46]. Classic helix and 2 teeth geometry has stress concentration problems at micro sizes. A chipped test tool is shown in Figure 4-3.

Figure 4-3 Chipped edge of a test tool

During inspection of the test tools showed that tool wear or chipping is always dominant on the one tooth. This can be seen in top views of the test tools as in the Figure 4-4.
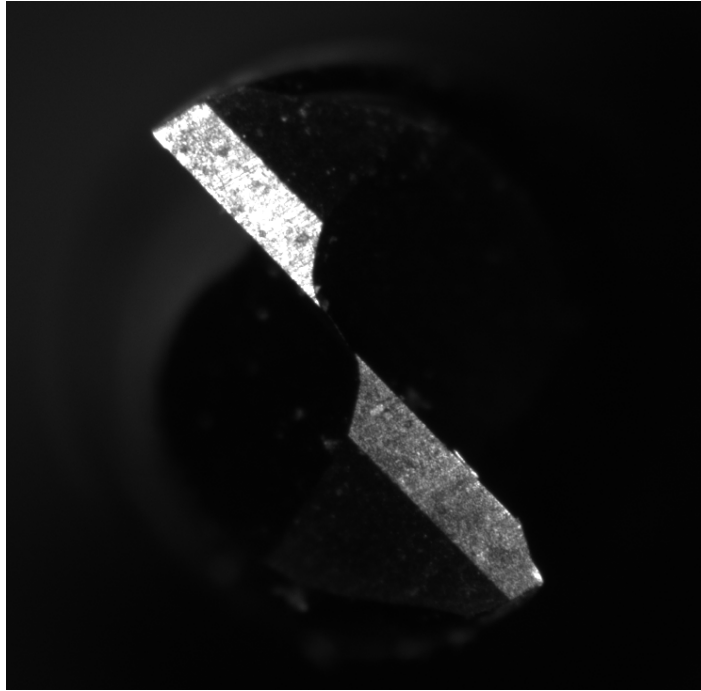
Figure 4-4 Dominant wear on one tooth

Tool run out (i.e. difference between geometrical center of the tool and the rotation center) is known to create this type of wears. And it is known that run-out to tool diameter ratio is higher in micro milling than macro milling.

4.2 Cutting Forces

Cutting forces are dependent on the tool geometry. Force to tool edge radius relation is studied before [28] [10] [22] [27]. Tool edge radius and its ratio to feed rate is the basic determining parameter in micro milling cutting forces. Feed rate to cutting force relations are accepted as linear in macro milling and its effect on the stability diagrams are generally considered as negligible. However, in micro milling scenarios, at low feed per tooth over cutter edge radius values, cutting forces become nonlinear. These effects are observed in the cutting force tests. In order to obtain a relation between cutting forces and tool edge radius measurement of edge radius and precise measurement of cutting forces are necessary. This type of a study is not done due to practical difficulties. After obtaining a reliable correlation between tool edge radius and cutting forces, the edge radius measurement should be done before stability tests. The

significance of this effect is seen in the following graphs. With increasing feed rates simulated cutting forces trends of simulated and measured cutting forces becomes similar. These simulations are done with Cutpro9 [44] and linear edge force model is used.

20um feed per tooth

20um feed per tooth

30um feed per tooth and slot milling

- - - Simulated Fx   —— Measured Fx
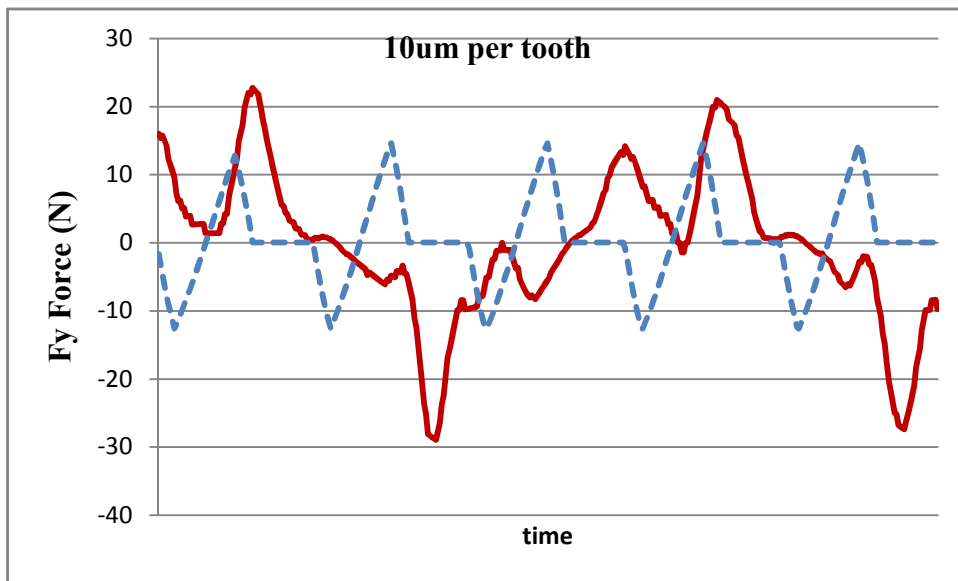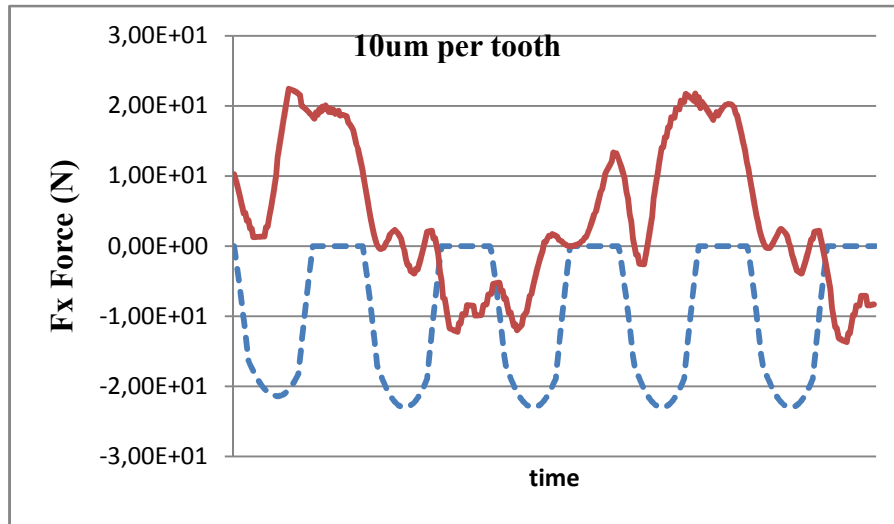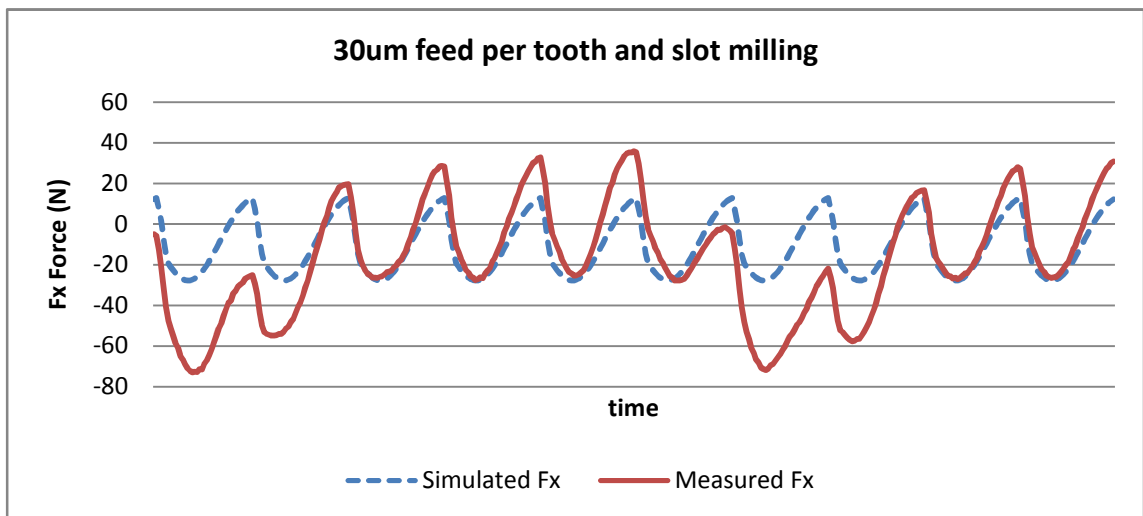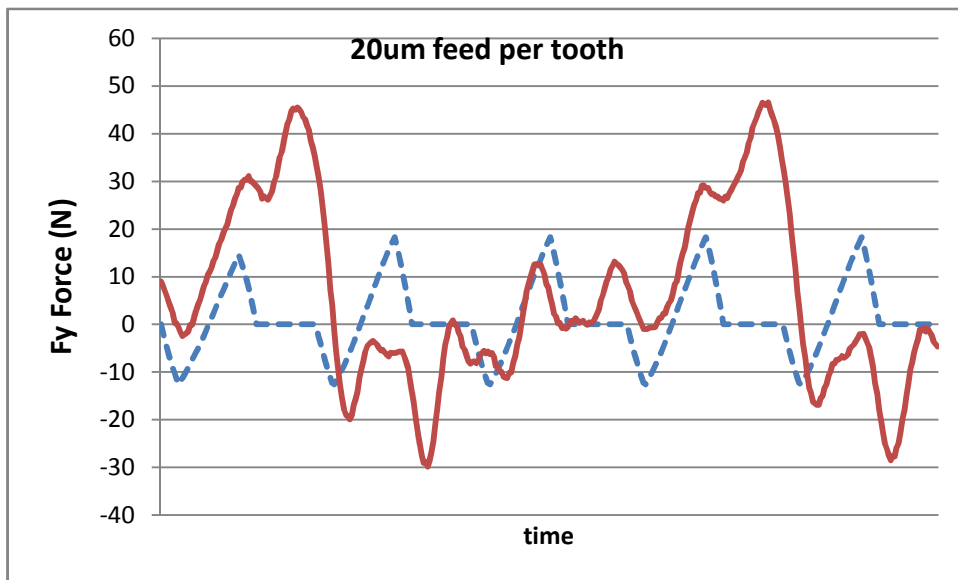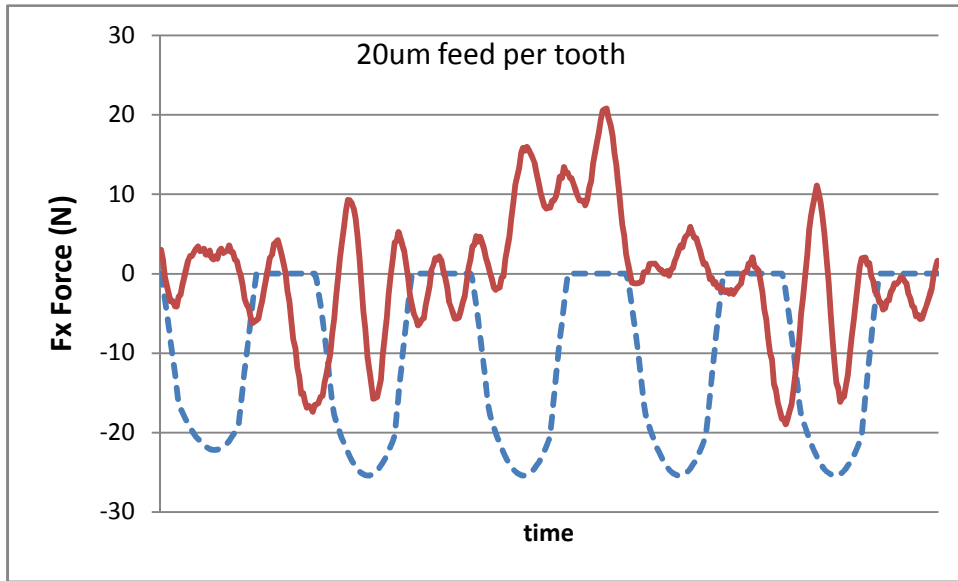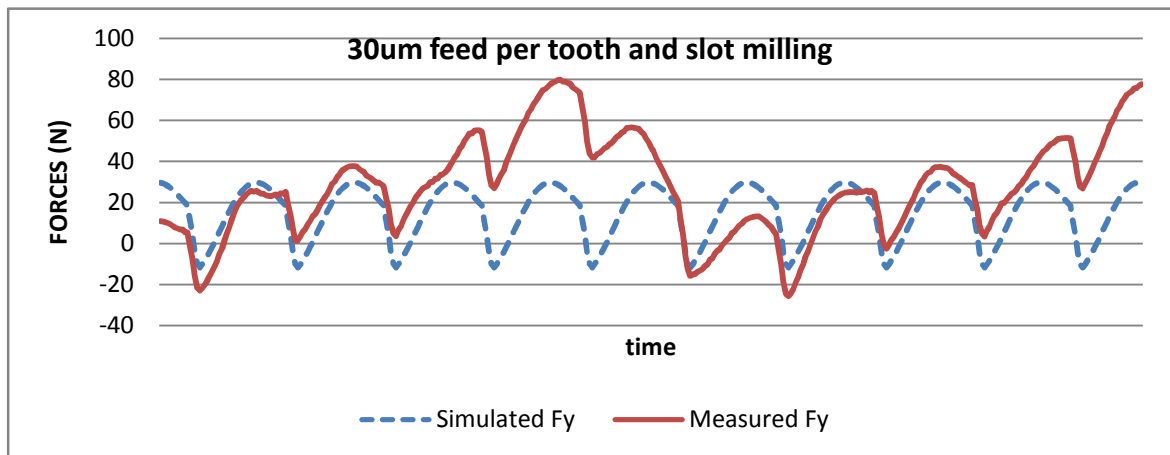
Figure 4-5 Force and Simulation trends with different feed rates and immersion depths

4.3   Tool Run-out in Miniature End Mills

The mainstream numerical and analytical modeling of machining approaches (see the section 1.2.3) are generally based on circular path approximation and the angles (i.e. rake angle, clearance angle) are defined with respect to the geometric center of the tool. The runout effects on instantaneous chip thickness and cutting forces are known and widely studied. These studies consider the radius change but not the changes in the cutter angles. Here true tool path effects on rake/clearance angles are presented:

4.3.1   Variable Angle Effects of Tool Run-Out

In conventional milling circular tool path approximation is common. Fundamental cutting angles are defined on an outer tangent circle to the tool edges (Figure 4-6). Rake and clearance angles are measured from rake and clearance surfaces to circle tangent and a perpendicular line to the tangent line at the tool edge point.
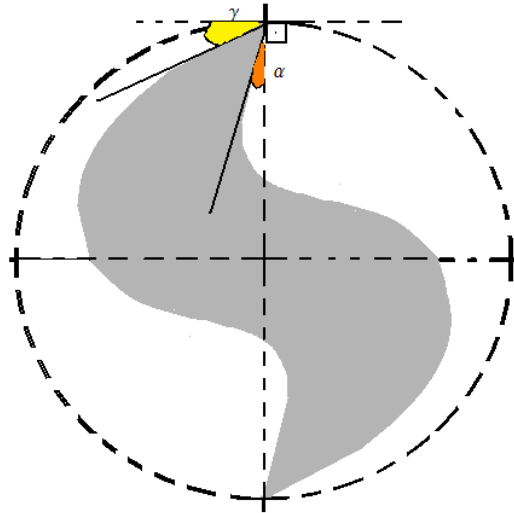
Figure 4-6 Rake and clearance angles defined on tool center

However, real path of the tool edge is not a circle and rotation center is not the center of outer tangent circle of the tool. Consider the run-out effect first which will be shown to be dominant. Run-out in plane is a 2-d vector and generally represented with an angle (β) and distance (ρ) between rotation center and tool center. Keeping the circular tool path assumption when the run-out introduced rake (α) and clearance(γ) angles changes in δα amount (Figure 4-7). It is not shown in the figure but this change means new rake angle becomes: α+ δα and clearance becomes γ - δα.
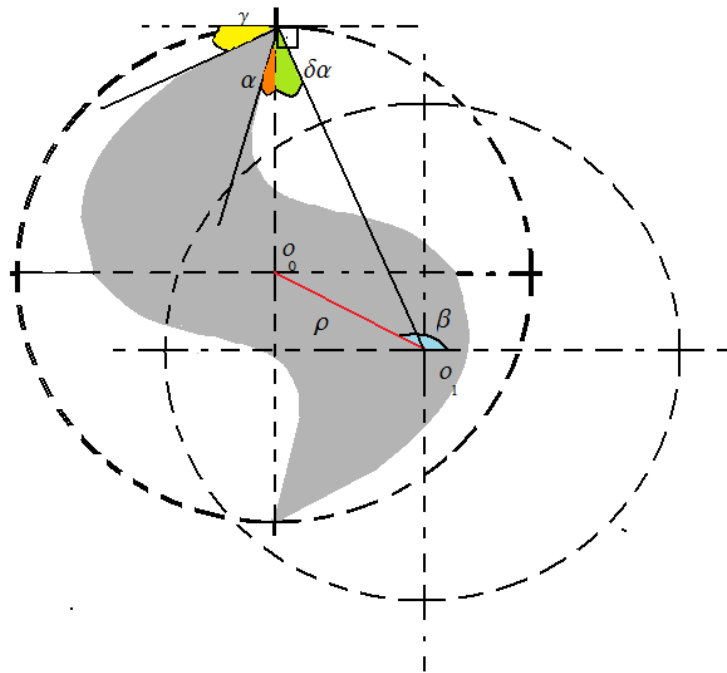
Figure 4-7 Run-out effects on angles

From another point of view run-out changes the tool diameter and it changes the angle difference between teeth (Figure 4-8). Change in the tool diameter is the parameter which is conventionally measured with dial gauges laser sensors etc. The phase difference (ϕ) introduced with the run-out is not easy to measure in a real tool. Change in effective radius can be measured. From measurement point of view another difficulty is run-out changes with rotational speed and measuring radius or diameter of the tool is another challenge.
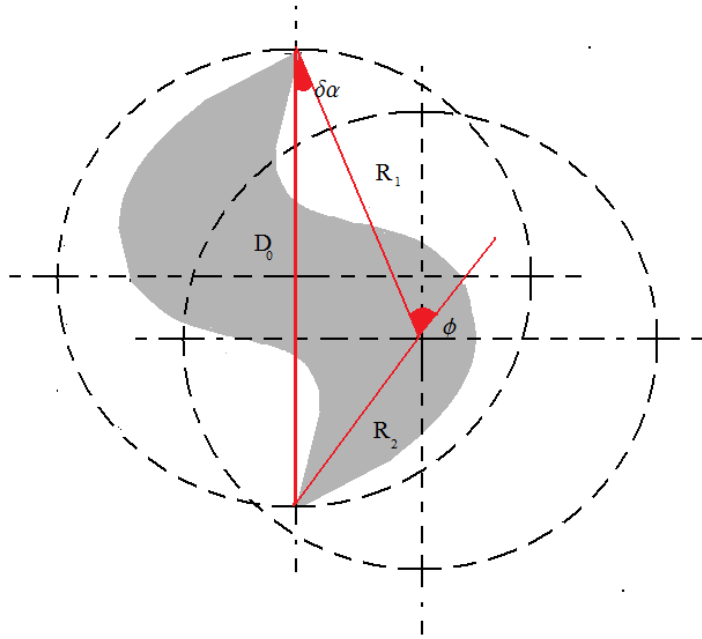
Figure 4-8 Run-out from observer's point of view

D_0 is known from tool diameter R_1, R_2 and ϕ can be measured at least when tool is not rotating. From cosine theorem:

$$\cos(\delta\,\alpha) = (R_1^2 + D_0^2 - R_2^2)/(2\,R_1 D_0) \qquad (4.3.1.1)$$

Run-out measurements show for the stability test conditions run-out is around 10 μm at its maximum. For different phase angles and run-out values change in the clearance and rake angles is shown in Figure 4-9. Results shows that for the test conditions change in rake and clearance angles are not significantly high. This change in the clearance angle should be checked with another study on process damping but according to the literature [3] change does not seem to create the discrepancy observed in the stability tests.
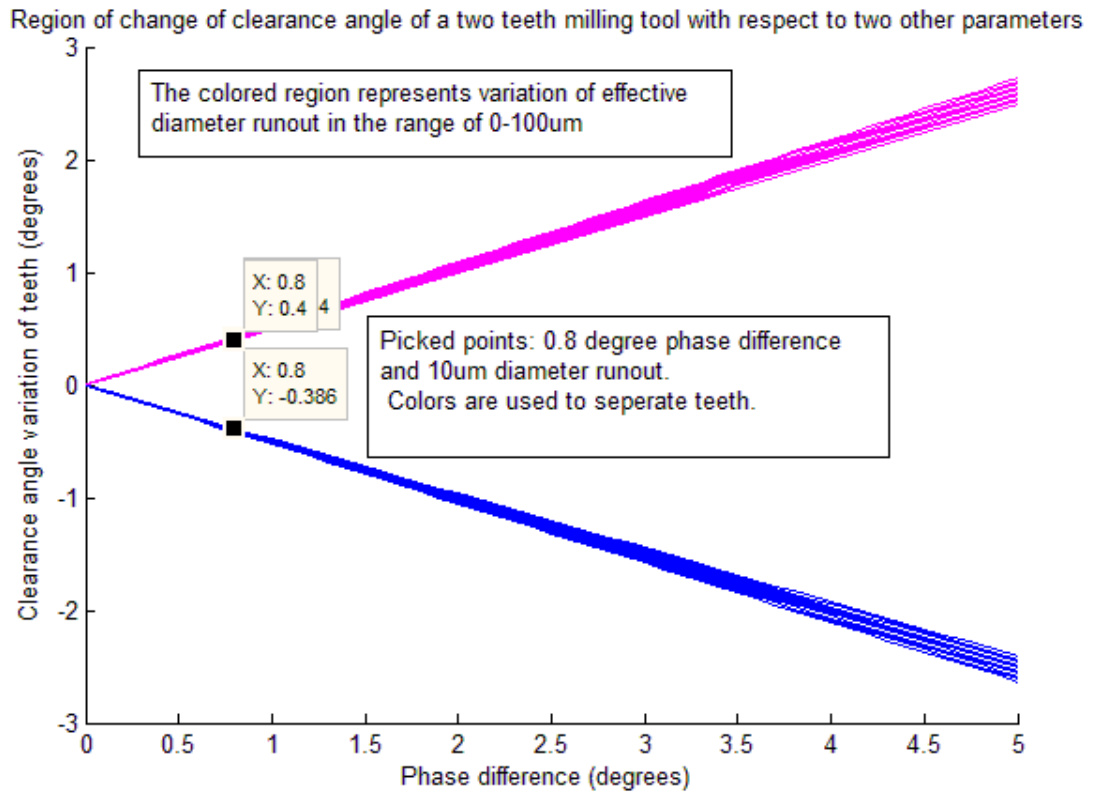
Figure 4-9 Change in clearance angle with run-out

Another parameter that changes the clearance angle is true tool path. Up to this point tool path is accepted as a circle. Actually it is a cycloid. And it can be represented as sum of two vectors A and R. A is translation vector and R is rotation vector. End of R vector creates tool path and tangent to the tool path and its normal is the true reference lines to define cutter angles. The difference between angles defined from rotation center (circular path assumption) and true tool path can be described as δα' in Figure 4-10.
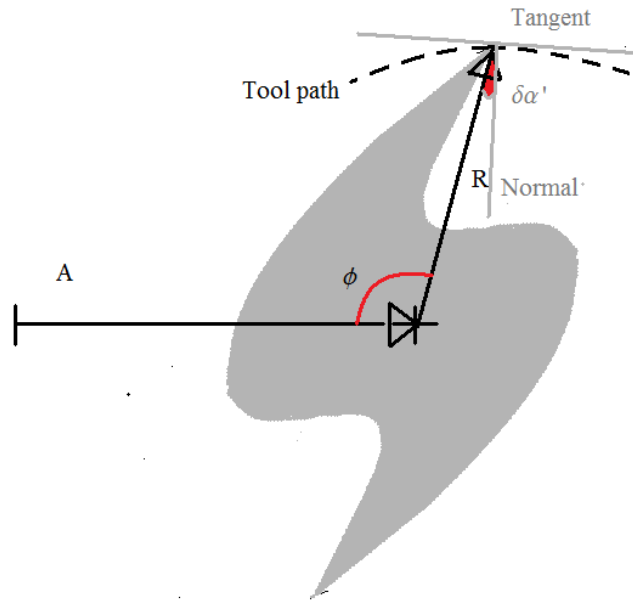
Figure 4-10 True tool path and change in the cutter angles.

Feed rate gives the relation between A and ϕ. For this geometry feed rate can be defined as rate of change of vector A and let N will be the number of teeth which is 2 for the figure. Let P is the tool path or trajectory of the cutter edge then:

$$A = \phi f N/(2\pi), \quad R = R\, e^{j\phi}, \quad P = \frac{\phi f N}{2\pi} + R\, e^{j\phi} \qquad (4.3.1.2)$$

Tangent is the derivative of the P.

$$\frac{\partial P}{\partial \phi} = \frac{fN}{2\pi} + j\, R\, e^{j\phi} \qquad (4.3.1.3)$$

The difference angle is sought and it can be found as:

$$\delta\alpha' = \phi - \arg\left(\frac{\partial P}{\partial \phi}\right) + \frac{\pi}{2} \qquad (4.3.1.4)$$

48

For the test conditions this difference variation area is numerically analyzed. Feed rate is defined as parametrically translation per revolution over tool diameter. Results can be seen in fig. Figure 4-11.
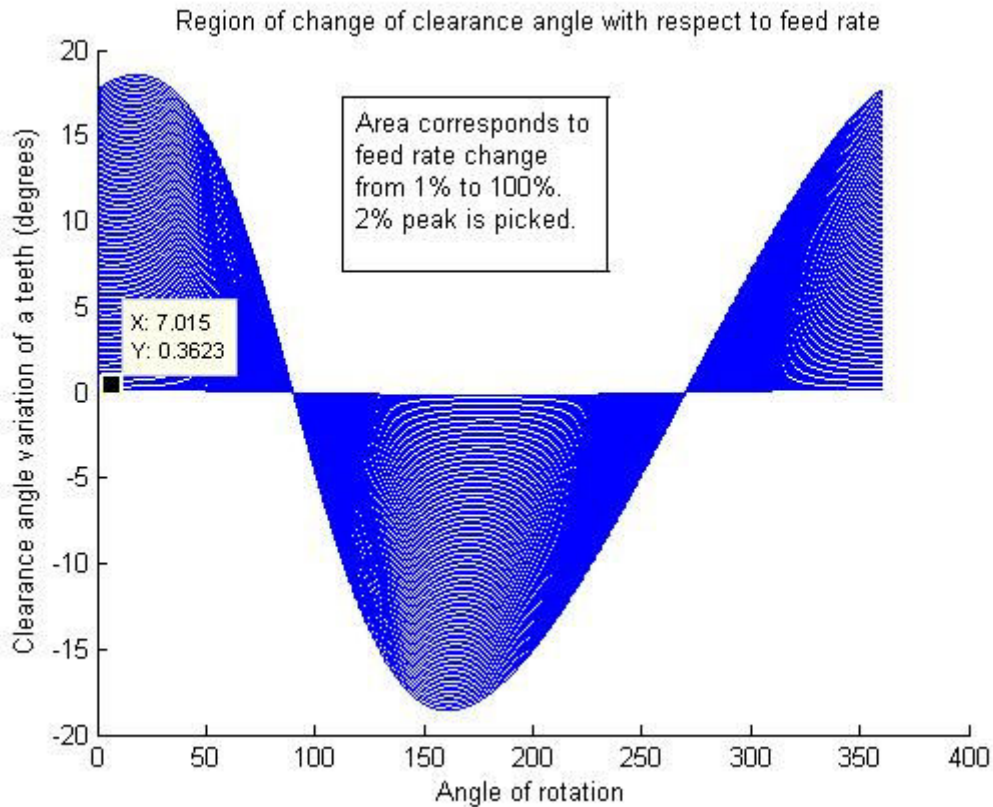
Figure 4-11 Feed rate effects on cutter angles

The total angle change from both run-out and feed rate contributions is around 0.7 degrees and it is not accepted as the main reason for the discrepancy of the stability limit prediction.

4.3.2 Time Domain Analysis Results with Tool Run-Out

This analysis done with the Cutpro9 software and it is aimed to see variable pitch effect of tool run-out. Change in the cutter angles are analyzed before and in this part change in the chip thicknesses of the teeth and phase differences of the teeth are analyzed to see that if their contribution on the stability limits are significant or not. This part of analysis was a main part of an ENS492 project [47] which is co-supervised by the author of this text. Their final simulation parameters are defined as identical to a

previous test scenario. And obtained results for the on machine test speeds are presented in Figure 4-12.
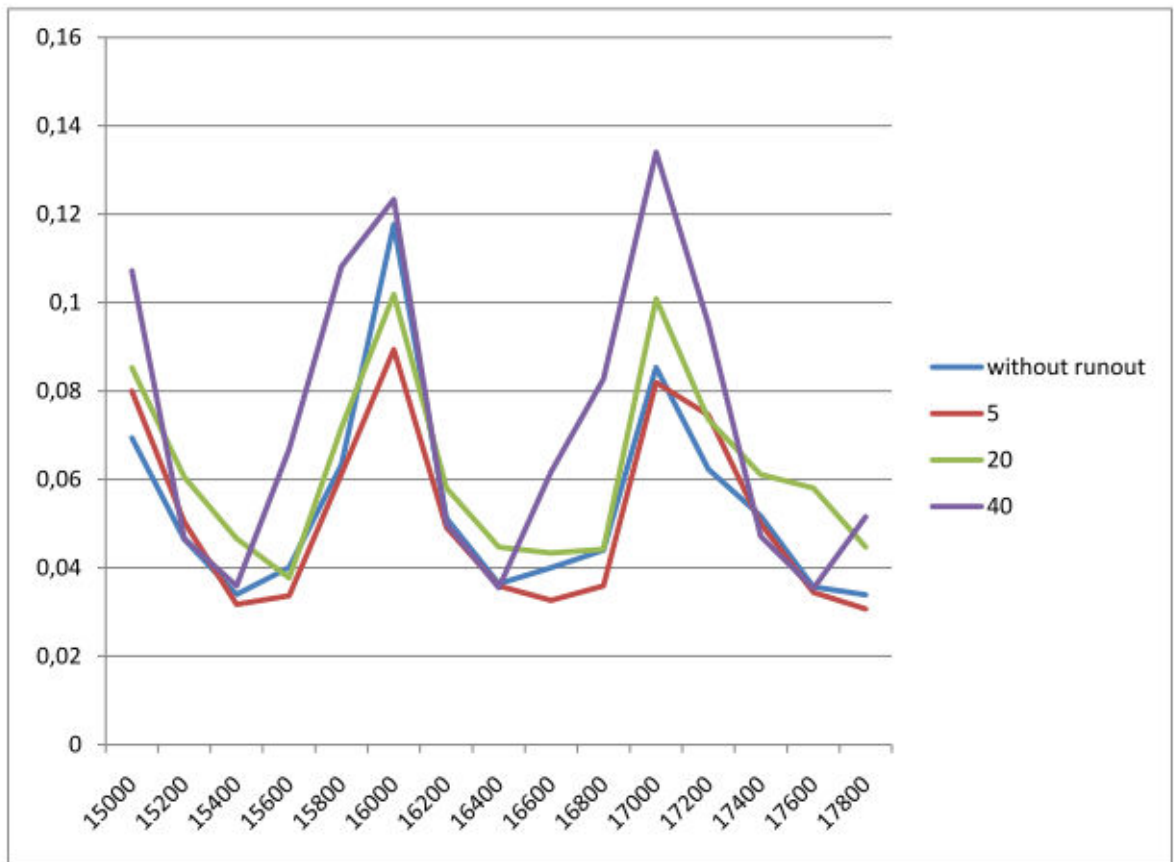
Figure 4-12 Stability limits found by time domain simulation with different tool run-out magnitudes (run-out values are in micrometer).

4.4   Deductions from Discrepancy Analysis

Tool run-out is analyzed in detail and it is seen that it was not the main reason. However, tool geometry inspection and cutting force fluctuations are reported [28] [11] to be causes of significant changes in stability limits. Micro milling cutting force coefficients are generally higher than the macro cutting coefficients. With the geometry factors shown in Figure 4-1, cutting coefficients become elevated and stability limits become far below the expected limits this makes it difficult to observe but if this is the case effects of chatter are so weak that it is not even easy to observe.
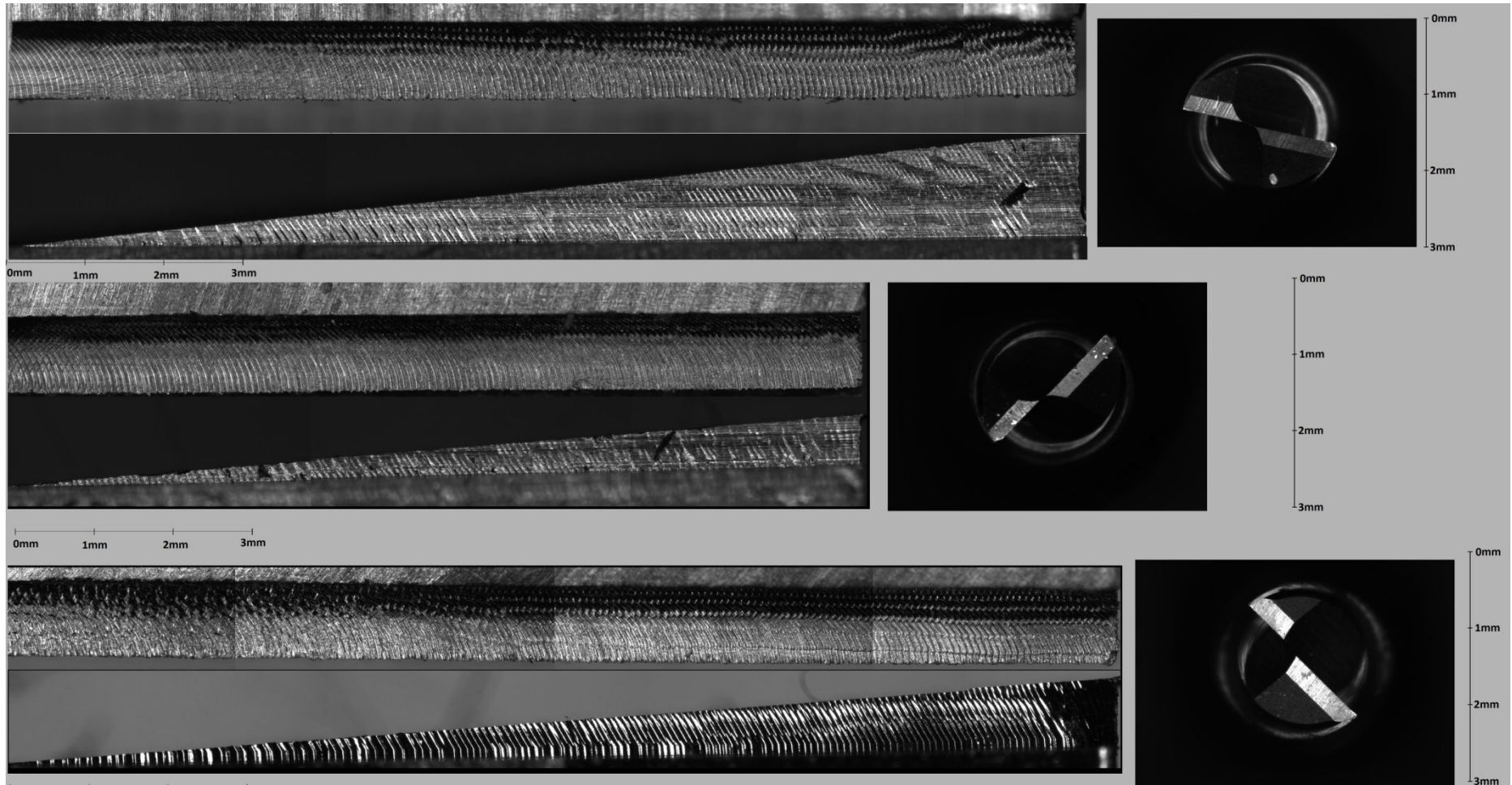
Figure 4-13 Ramp test surfaces and tested tools. Top: Unused tool with one rake Middle: Chipped tool with one rake Bottom: Unused tool with two rake

51

Another reason is undesirable cutting conditions. When tool diameter is considered high feed rates are used in order to reduce the edge force contributions on the total cutting force. Higher feed rates resulted in excessive chip load on the tool edge and almost all tests are ended with a chipped end corner of the tool. Chipped end corner is a source of non-cutting a rubbing condition instead of desired shearing. Such a rubbing mechanism is also a source of damping or energy dissipation during tool vibration. This variation is tested with different tools (Figure 4-13). Three tools having same overhang length of 27mm are used. Same torques were applied during clamping. The test material was 7075 aluminum. Difference between bottom surface marks shows that vibration amplitudes are reduce in the chipped tool. However second rake lowered stability limit and vibration amplitudes become higher. Thus chipped edge results in elevated stability limits which are far beyond the expectations of the analytical model.

CHAPTER 5 CONCLUSION

5.1   Summary and Contribution

The dynamics and stability of miniature milling tools were investigated in this study. An indirect measurement method is used for the identification of tool point FRF. The proposed method is a practical approach for measurement dynamics of miniature tools. However, there may be some errors due to the excitation and noise. Noise amplification can be filtered by source data modal fitting. Tool shank excitation for higher frequencies can also accomplished by high frequency shakers. Since proposed method allows exciting stiffer parts of the structure, shaker excitation modal tests can also be used for miniature tools.

Ultimate aim of the tool dynamics analysis is to determine the stability limits which are obtained using the analytical stability model of Budak and Altintas [2]. Experimental verification for the stability limits was tried with little success. Various stability tests with different spindle speeds and cutting depths shows that the detection of chatter is very difficult, and in many cases it is not possible using the standard methods such as sound and vibration measurement or surface inspection. Expected vibration amplitudes of tool tip are around tens of microns. These values may be so small to detect with the available equipment and from practical stand-off distances. Tool geometry, cutting forces and tool run-out are analyzed as causes of the discrepancy. However analysis results shows the main causes can be tool geometry or cutting force. Process damping [11] and multi-frequency chatter [42] effects may contribute the discrepancies observed as well. Stability prediction of micro end mills needs further investigation.

5.2   Future Work

Micro milling run-out effects are studied from a common point view in the literature. Chip thickness change is modeled extensively but clearance angle changes and process damping effects of run-out still remains undefined.

It is seen that indirect measurements have frequency limitations in terms of excitation. Miniature impact hammers are used to excite frequencies up to 10 kHz. Another difficulty is about tool sizes. Measuring tip vibration in tools having 100 micrometer diameter needs special equipments and it is beyond MRL's current LDV capabilities. Receptance coupling method is the common path in the literature for micro milling dynamics prediction. Most of the receptance coupling studies need parameter identification and their repeatability is low. Micro milling Receptance coupling method should be a test based method in order to be accurate and reliable with the expense of less practicality.

CHAPTER 6 APPENDIX

6.1 Modal Data Extraction For Curve Fitting
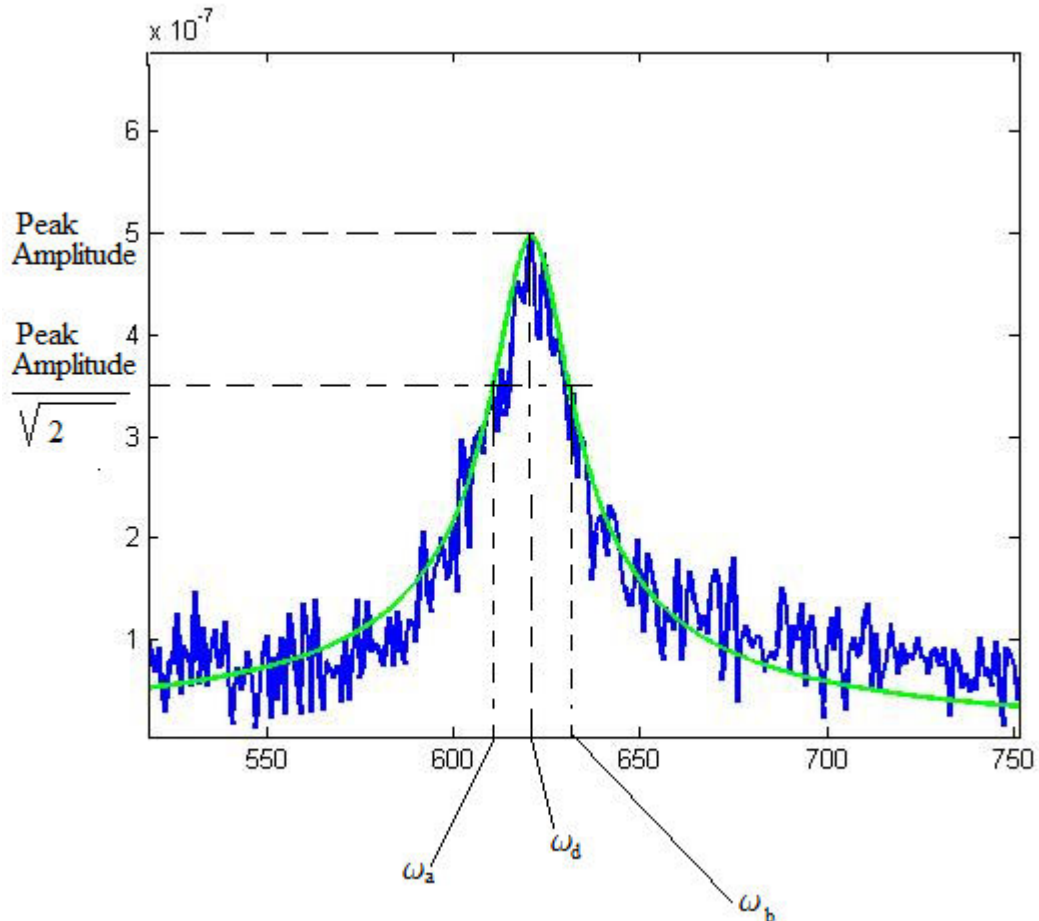
Figure 6-1Curve fitting method

In order to filter the noises and cancel the anti-mode effects a modal parameter identification method [37] is used.

The method uses amplitude and frequency information. Let G is the transfer function of the system. The peak value at the mode shape ($G(\omega_d)$) determines the damped natural frequency (ω_d) (Figure 6-1). And the damping ratio found by:

$$G^{-1}\left(G(\omega_d)\Big/\sqrt{2}\right) = \omega_a, \omega_b \qquad (6.1.1)$$

Then,

$$\xi = \frac{\omega_a - \omega_b}{2\,\omega_d}$$

(6.1.2)

Natural frequency is defined as:

$$\omega_n = \omega_d \sqrt{1 - \xi^2}$$

(6.1.3)

Modal stiffness, using the peak value, can be found as follows:

$$k = \left[\frac{\omega_n^2}{\sqrt{(\omega_n^2 - \omega_d^2)^2 + (2\xi\omega_d\omega_n)^2}}\right] |G(\omega_d)|^{-1}$$

(6.1.4)

With all these parameters transfer function can be reconstructed as follows:

$$G(\omega) = \left[\frac{\omega_n^2}{\sqrt{(\omega_n^2 - \omega^2)^2 + (2\xi\omega\omega_n)^2}}\right] k^{-1}$$

(6.1.5)

6.2   List of Tested Milling Conditions for Chatter Detection

Table 6-1 List of Stability conditions

3mm tool (radial depth 0,2 mm)

axial depth of cut (mm)	Spindle Speed (rpm)	feed per tooth (mm)	number of teeth	feed mm/min	Vcut (mm/min)
0,10	12500,00	0,05	4,00	2500,00	117,81
0,15	12500,00	0,05	4,00	2500,00	117,81
0,20	12500,00	0,05	4,00	2500,00	117,81
0,25	12500,00	0,05	4,00	2500,00	117,81
0,10	11000,00	0,05	4,00	2200,00	103,67
0,15	11000,00	0,05	4,00	2200,00	103,67
0,20	11000,00	0,05	4,00	2200,00	103,67
0,25	11000,00	0,05	4,00	2200,00	103,67
2mm tool flexible workpiece (radial depth 0,1 mm)					
0,05	14325,00	0,04	2,00	1146,00	90,01
0,08	14325,00	0,04	2,00	1146,00	90,01
0,10	14325,00	0,04	2,00	1146,00	90,01
0,13	14325,00	0,04	2,00	1146,00	90,01
0,40	14325,00	0,04	2,00	1146,00	90,01
2mm tool airturbine (radial depth 0,1 mm)					
0,05	33000,00	0,02	4,00	2640,00	207,35
0,10	33000,00	0,02	4,00	2640,00	207,35
0,15	33000,00	0,02	4,00	2640,00	207,35
0,20	33000,00	0,02	4,00	2640,00	207,35
2mm (radial depth 0,1 mm)					
0,15	10250,00	0,04	2,00	820,00	64,40
0,20	10250,00	0,04	2,00	820,00	64,40
0,25	10250,00	0,04	2,00	820,00	64,40
0,30	10250,00	0,04	2,00	820,00	64,40
0,35	10250,00	0,04	2,00	820,00	64,40
0,40	10250,00	0,04	2,00	820,00	64,40
0,60	10250,00	0,04	2,00	820,00	64,40
0,60	10000,00	0,04	2,00	800,00	62,83
0,60	10500,00	0,04	2,00	840,00	65,97
1,00	10250,00	0,04	2,00	820,00	64,40
1,00	15500,00	0,04	2,00	1240,00	97,39
0,80	10000,00	0,04	2,00	800,00	62,83
1,00	10000,00	0,04	2,00	800,00	62,83
1,20	10000,00	0,04	2,00	800,00	62,83
0,80	10000,00	0,04	2,00	800,00	62,83
0,60	10000,00	0,04	2,00	800,00	62,83

0,60	10100,00	0,04	2,00	808,00	63,46
0,60	10100,00	0,04	2,00	808,00	63,46
0,60	10250,00	0,04	2,00	820,00	64,40
0,80	10250,00	0,04	2,00	820,00	64,40
1,00	10250,00	0,04	2,00	820,00	64,40
1,20	10250,00	0,04	2,00	820,00	64,40
1,50	10250,00	0,04	2,00	820,00	64,40
0,20	17300,00	0,04	2,00	1384,00	108,70
0,40	17300,00	0,04	2,00	1384,00	108,70
0,10	17300,00	0,04	2,00	1384,00	108,70
0,60	17300,00	0,04	2,00	1384,00	108,70
0,60	17300,00	0,04	2,00	1384,00	108,70
0,60	16600,00	0,04	2,00	1328,00	104,30
0,40	16600,00	0,04	2,00	1328,00	104,30
0,50	16600,00	0,04	2,00	1328,00	104,30
0,70	16600,00	0,04	2,00	1328,00	104,30
1,00	16600,00	0,04	2,00	1328,00	104,30
1,20	16600,00	0,04	2,00	1328,00	104,30
0,10	16600,00	0,04	2,00	1328,00	104,30
2,00	16600,00	0,04	2,00	1328,00	104,30
1,60	16600,00	0,04	2,00	1328,00	104,30
1,40	16600,00	0,04	2,00	1328,00	104,30
2mm tool radial depth 1mm					
0,60	15600,00	0,04	2,00	1248,00	98,02
0,50	15600,00	0,04	2,00	1248,00	98,02
0,40	15600,00	0,04	2,00	1248,00	98,02
0,30	15600,00	0,04	2,00	1248,00	98,02
0,20	15600,00	0,04	2,00	1248,00	98,02
0,10	15600,00	0,04	2,00	1248,00	98,02
1,00	15600,00	0,04	2,00	1248,00	98,02
0,90	15600,00	0,04	2,00	1248,00	98,02
0,80	15600,00	0,04	2,00	1248,00	98,02
0,70	15600,00	0,04	2,00	1248,00	98,02
1,00	16700,00	0,04	2,00	1336,00	104,93
0,90	16700,00	0,04	2,00	1336,00	104,93
0,80	16700,00	0,04	2,00	1336,00	104,93
0,70	16700,00	0,04	2,00	1336,00	104,93
0,60	16700,00	0,04	2,00	1336,00	104,93
0,50	16700,00	0,04	2,00	1336,00	104,93
0,40	16700,00	0,04	2,00	1336,00	104,93
0,30	16700,00	0,04	2,00	1336,00	104,93
0,20	16700,00	0,04	2,00	1336,00	104,93

CHAPTER 7   BIBLIOGRAPHY

1. **Altintas, Y.** *Manufacturing Automation.* s.l. : Cambridge University Press, 2000.

2. *Analytical Prediction of Chatter Stability in Milling—Part I: General Formulation.* **E. Budak, and Y. Altintas.** 1998, ASME Journal of Dynamic Systems, pp. 22-30.

3. *Chatter suppression in micro end milling with process damping.* **R. Rahnama, M. Sajjadi, S. Park.** s.l. : Journal of Materials Processing Technology, 2009, Vol. 209, pp. 5766–5776.

4. **T. Schmitz, S. Smith.** *Machining Dynamics: Frequency Response to Improved Productivity.* s.l. : Springer, 2009.

5. *Analytical modeling of spindle-tool dynamics on machine tools using Timoshenko beam model and receptance coupling for the prediction of tool point FRF.* **A. Ertürk, H.N. Özgüven, Budak E.** 15, s.l. : International Journal of Machine Tools and Manufacture, 2006, Vol. 46.

6. *A spectral-Tchebychev technique for solving linear and nonlinear beam equations.* **S. Filiz, O.B. Ozdoganlar and L.A. Romero.** 8, s.l. : Journal of Vibration and Controls, 2008, Vol. 14.

7. *"Substructure Coupling of Micro-end mills to Aid in the Suppression of Chatter".* **Mascardelli, B., Park, S.S., Freiheit, T.** s.l. : ASME Transactions, Journal of Manufacturing Science and Engineering, 2008, Vol. 130.

8. *Structural modeling of end mills for form error and stability analysis.* **E.B. Kivanc, E. Budak.** s.l. : International Journal of Machine Tools and Manufacture, 2004, Vol. 44 .

9. *Indirect Measurement of Multiple Excitation Force Spectra by FRF Matrix Inversion: Influence of Errors in Statistical Estimates of FRFs and Response Spectra.* **M.Blau.** s.l. : Acta Acustica united with Acustica, 1999-07-01, Vol. 85.

10. *Extension of cutting force formulae for microcutting.* **J. Fleischer, V. Schulze, J. Kotschenreuther.** s.l. : CIRP Journal of Manufacturing Science and Technology, 2009.

11. *Chatter suppression in micro end milling with process damping.* **Ramin Rahnama, Mozhdeh Sajjadi, Simon S. Park.** s.l. : Journal of Materials Processing Technology, 2009, Vol. 209.

12. *Robust chatter stability in micro-milling operations.* **S.S. Park, R. Rahnama.** s.l. : CIRP Annals - Manufacturing Technology, 2010, Vol. 59.

13. *State of Art of the Micromachining.* **T., Masuzawa.** 2, s.l. : CIRP Annals - Manufacturing Technology, Vol. 49.

14. *Current status in, future trends of, ultraprecision machining and ultrafine materials.* **Taniguchi, N.** s.l. : Annals of the CIRP, 1983.

15. *Recent Advances in Mechanical Micromachining.* **D. Dornfeld, S. Min, Y. Takeuchi.** 2, s.l. : CIRP Annals - Manufacturing Technology, 2006, Vol. 55.

16. *Creation of 3-D tiny statue by 5-axis control ultraprecision machining.* **Y. Takeuchi, H. Yonekura, K. Sawada.** s.l. : Computer Aided Design, 2003, Vol. 35.

17. *Probe-Based 3-D Nanolithography Using Self-Amplified Depolymerization Polymers.* **Armin W. Knoll, David Pires, Olivier Coulembier, Philippe Dubois , James L. Hedrick ,.** s.l. : Advanced Materials, 2010, Vol. 22.

18. *Modeling micro-end-milling operations. Part 1: analytical cutting force model.* **W. Y. Bao, I. N. Tansel.** 15, s.l. : International Journal of Machine Tools and Manufacture, 2000, Vol. 40.

19. *Empirical analysis of cutting force constants in micro-end-milling operations .* **G. Newby, S. Venkatachalam, and S.Y. Liang.** s.l. : Journal of Materials Processing Technology, 2007, Vol. 192.

20. *Investigation of the Dynamics of Micro-end Milling Part 1: Model Development.* **Jun MBG, Liu X, deVor RE, Kapoor SG.** 4, s.l. : Transactions of ASME Journal of Manufacturing Science and Engineering, 2006, Vol. 128.

21. *Mechanistic modeling and accurate measurement of micro end milling forces.* **S.S. Park, M. Malekian.** s.l. : CIRP Annals - Manufacturing Technology, 2009, Vol. 58.

22. *Tooling Structure: Interface between Cutting Edge and Machine Tool .* **Eugene I, Rivin.** 49, s.l. : Annals of the ClRP , 2000.

23. *"The Effects of Run-Out on Cutting Geometry and Forces in End Milling".* **Kline, W.A., DeVor, R.E.** s.l. : International Journal of Machine Tool Design and Research, 1983, Vol. 23.

24. *Computerized Predictive Cutting Models for Forces in End-Milling Including Eccentricity Effects.* **E.J.A. Armarego, N.P. Deshpande.** 1, s.l. : CIRP Annals - Manufacturing Technology, 1989, Vol. 38.

25. *Modeling micro-end-milling operations. Part II: tool run-out.* **W.Y. Bao, I.N. Tansel.** s.l. : International Journal of Machine Tools & Manufacture, 2000, Vol. 40.

26. *Modelling and simulation of micro-milling cutting forces.* **S.M. Afazov, S.M. Ratchev, J. Segal.** s.l. : Journal of Materials Processing Technology, 2010.

27. *Effects of the Cutting Tool Edge Radius on the Stability Lobes in Micro-milling.* **AFAZOV, S., RATCHEV, S. and SEGAL, J.,.** s.l. : Advanced Materials Research, 2011, Vol. 223.

28. *Predicting High-Speed Machining Dynamics by Substructure Analysis.* **Schmitz, T. and Donaldson, R.** 1, s.l. : Annals of the CIRP, 2000, Vol. 49.

29. *Tool Point Frequency Response Prediction for High-Speed Machining by RCSA.* **Tony L. Schmitz, Matthew A. Davies, Michael D. Kennedy.** s.l. : Transactions of the ASME, 2001, Vol. 123.

30. *The Analysis of Vibrating Systems which Embody Beams .* **Bishop, R. E. D.** s.l. : Proceedings of the Institution of Mechanical Engineers 1847-1996, 1955, Vol. 169.

31. *Receptance coupling for end mills.* **Simon S. Park, Yusuf Altintas and Mohammad Movahhedy.** 9, s.l. : International Journal of Machine Tools and Manufacture, 2003, Vol. 43.

32. *Analytical modeling of spindle–tool dynamics on machine tools using Timoshenko beam model and receptance coupling for the prediction of tool point FRF.* **Budak, A. Ertürk N. Özgüven E.** s.l. : International Journal of Machine Tools & Manufacture, 2006, Vol. 46.

33. *Timoshenko Beam-Column with Generalized End Conditions and Nonclassical Modes of Vibration of Shear Beams.* **Aristizabal-Ochoa, J. Dario.** s.l. : JOURNAL OF ENGINEERING MECHANICS, 2004.

34. *A spectral-Tchebychev technique for solving linear and nonlinear beam equations.* **Baris Yagcı, Sinan Filiz, Louis L. Romero, O. Burak Ozdoganlar.** s.l. : Journal of Sound and Vibration, 2009.

35. *A three-dimensional model for the dynamics of micro-endmills including bending, torsional and axial vibrations.* **Sinan Filiz, O. Burak Ozdoganlar.** 1, s.l. : Precision Engineering, 2011, Vol. 35.

36. **Jimin He, Zhi-Fang Fu.** *Modal Analysis,.* s.l. : Butterworth-Heinemann , 2000.

37. *Engineering Vibration.* **D., Inman J.** s.l. : Prentice-Hall , 2001.

38. **Cheng, Kai.** *Machining Dynamics: Fundamentals, Applications and Practices.* s.l. : Springer , 2008.

39. *Multi Frequency Solution of Chatter Stability for Low Immersion Milling.* **Altintas, S. D. Merdol and Y.** s.l. : J. Manuf. Sci. Eng., 2004.

40. *Chatter stability of milling in frequency and discrete time domain.* **Y. Altintas, G. Stepan, D. Merdol and Z. Dombovari.** 1, s.l. : CIRP Journal of Manufacturing Science and Technology, 2008, Vol. 1.

41. **Cutpro 9 sofware, MAL Inc. (last update at December 2010).**

42. *Detecting and identifying artificial acoustic emission signals in an industrial fatigue environment.* **J. Hensman, R. Pullin, M. Eaton, K. Worden, K.M. Holford, S.L. Evans.** 4, s.l. : Meas. Sci. Technol., (2009), Vol. 20.

43. *Tool geometry study in micromachining.* **F.Z. Fang, H. Wu, X.D. Liu, Y.C. Liu, S.T. Ng.** s.l. : Journal of Micromechanics and Microengineering, 2003, Vol. 13.

44. **Çağlar Özdemir, Oğuzhan Bahçıvan, Öncü Güneş Atar.** *#045 Investigation of Micro Milling Process Dynamics and Stability .* 2011.